HELSINKI UNIVERSITY OF TECHNOLOGY

Department of Electrical and Communications Engineering

Sampo Pitkänen

Optimal reception of 64 Quadrature Amplitude Modulation in High-Speed Downlink Packet Access

Salo, Finland, January 2nd, 2008

Supervisor of the Thesis: Professor   Olli Simula

Instructor of the Thesis: Lic. Tech.   Timo Huuhtanen

HELSINKI UNIVERSITY OF TECHNOLOGY	ABSTRACT OF THE MASTER'S THESIS
Author: Sampo Pitkänen	
Name of the Thesis: Optimal reception of 64 Quadrature amplitude modulation in High-Speed Downlink Packet Access	
Date: January 2nd, 2008	**Number of pages:** 78
Department of Electrical and Communications Engineering **Professorship:** T-115 Computer and Information Science	
Supervisor: Professor Olli Simula **Instructor:** Lic. Tech. Timo Huuhtanen	

High-speed downlink packet access (HSDPA) is a feature introduced to the universal mobile telecommunications system (UMTS) in 2002. It allows data rates of up to 14.4 Mbps in the downlink. In 2007 new features were standardized to HSDPA, including 64 Quadrature Amplitude Modulation (64-QAM).

64-QAM allows more data to be transmitted on the same bandwidth, increasing the HSDPA peak data rate to 21.6 Mbps. Transmitters and receivers must be updated with new algorithms to support this new modulation type. On the terminal side the amplitude of the signal must first be precisely estimated so that it can be demodulated correctly. Then a demodulation algorithm with good enough accuracy must be applied. Similar algorithms were already used with older HSDPA versions, but 64-QAM is much more sensitive to errors.

In this thesis, three amplitude estimation and three demodulation algorithm candidates were considered. A physical layer HSDPA simulator with realistic parameters was used to compare the algorithms.

There was no clear winner when selecting the best way to estimate the amplitude, but two of the algorithm candidates proved to be better than the third. The best demodulation algorithm for practical applications turned out to be a simplified MAP optimum detector that models the demodulation as a one-dimensional problem.

Keywords: 3G, WCDMA, HSDPA, 64-QAM, demodulation

TEKNILLINEN KORKEAKOULU	DIPLOMITYÖN TIIVISTELMÄ

Tekijä: Sampo Pitkänen	
Työn nimi: 64-QAM –signaalin optimoitu vastaanottomenetelmä HSDPA:ssa	
Päivämäärä: 2. tammikuuta 2008	**Sivumäärä:** 78

Sähkö- ja tietoliikennetekniikan osasto

Professuuri: T-115 Informaatiotekniikka

Työn valvoja: Professori   Olli Simula

Työn ohjaaja: Tek. Lisensiaatti   Timo Huuhtanen

HSDPA on vuonna 2002 UMTS-verkkoihin lisätty ominaisuus. Sen avulla laskevalla siirtotiellä mobiililaitteiden huippunopeudeksi saadaan 14.4 megabittiä sekunnissa. Vuonna 2007 standardoitiin uusia HSDPA-ominaisuuksia, niiden mukana uusi modulaatiotyyppi 64-QAM.

64-QAM:in avulla suurin siirtonopeus saadaan nostettua 21.6:n megabittiin sekunnissa. Sekä lähettimiä että vastaanottimia on päivitettävä uuden modulaatiotyypin tukemiseksi. Vastaanottopäässä signaalin amplitudi täytyy ensin estimoida tarkasti jotta signaali voidaan vastaanottaa oikein. Signaali pitää vielä tämän jälkeen demoduloida riittävällä tarkkuudella. Samankaltaisia algoritmeja on käytetty jo vanhemmissa HSDPA-versioissa, mutta 64-QAM on huomattavasti herkempi virheille.

Tässä työssä amplitudiestimointia ja demodulointia varten testattiin kolmea eri algoritmivaihtoehtoa. Algoritmien vertailuun käytettiin fyysisen kerroksen HSDPA-simulaattoria, jossa käytettiin standardin mukaisia realistisia parametreja.

Lopputuloksena yksiselitteisesti parasta tapaa estimoida amplitudia ei löytynyt, mutta kaksi ehdokkaista osoitti hyviä ominaisuuksia. Parhaaksi demodulointialgoritmiksi osoittautui yksinkertaistettu versio optimaalisesta MAP-ilmaisimesta, joka hoitaa demoduloinnin yksiulotteisesti.

Avainsanat: 3G, WCDMA, HSDPA, 64-QAM, demodulointi

PREFACE

This thesis was written for the Modem System Design team in the Technology Platforms organization of Nokia.

I would like to thank my instructor and manager Timo Huuhtanen for continuous support and for allowing me time to finish my thesis. I would also like to thank my supervisor Olli Simula, who always responded quickly to all questions.

I would also like to thank all my colleagues at Nokia, especially Keijo Möttönen who always had an answer for almost any question. Kalle Tuulos and Maarit Melvasalo also gave plenty of good feedback.

Salo, Finland, January 2nd, 2008

Sampo Pitkänen

INDEX

FIGURE INDEX

TABLE INDEX

LIST OF ABBREVIATIONS

16-QAM	16 Quadrature Amplitude Modulation
2G	2nd generation, refers to second generation (digital) mobile phone systems like GSM and US TDMA. Used typically when e.g. the GSM hardware is referenced in general, like "2G baseband logic"
3G	3rd generation, refers to the third generation mobile phone systems like the WCDMA
3GPP	3rd Generation Partnership Project
64-QAM	64 Quadrature Amplitude Modulation
8PSK	8 Phase Shift Keying
ACK	Acknowledgement
AICH	Acquisition Indication Channel
AMC	Adaptive Modulation and Coding
ARQ	Automatic Repeat Request.
AWGN	Additive White Gaussian Noise
BCH	Broadcast Channel
BER	Bit Error Rate
BLER	Block Error Rate
BMC	Broadcast/Multicast Control Protocol
BTS	Base Transceiver Station
BPSK	Binary Phase Shift Keying
C-Plane	Control Plane
CAI	Channel Assignment Indicator
CCTrCh	Coded Composite Transport Channel
CD/CA-ICH	Collision Detection/Channel Assignment Indicator Channel
CDI	Collision Detection Indicator
CDMA	Code Division Multiple Access
CN	Core Network

CPCH	Uplink Common Packet Channel
CPICH	Common Pilot Channel
CQI	Channel Quality Information
CRC	Cyclic Redundancy Check
CSICH	CPCH Status Indication Channel
DCH	Dedicated Channel
DPCCH	Dedicated Physical Control Channel
DPCH	Dedicated Physical Channel
DPDCH	Dedicated Physical Data Channel
DPP	Decision Point Power
DSCH	Downlink Shared Channel
E-AGCH	E-DCH Absolute Grant Channel
E-DCH	Enhanced DCH
E-DPCCH	Enhanced DPCCH
E-DPDCH	Enhanced DPDCH
E-HICH	E-DCH Hybrid ARQ Indicator Channel
E-RGCH	E-DCH Relative Grant Channel
EDGE	Enhanced Data Rate for GSM evolution
F-DPCH	Fractional Dedicated Physical Channel
FACH	Forward Access Channel
FDD	Frequency Division Duplex
G	Geometry
GERAN	GSM EDGE Radio Access Network
GPRS	General Packet Radio Service
GSM	Global System for Mobile Communication
HARQ	Hybrid-ARQ
HSCSD	High-Speed Circuit Switched Data
HSDPA	High-Speed Downlink Packet Access

HS-DPCCH	High-Speed Dedicated Physical Control Channel
HS-DSCH	High-Speed Downlink Shared Channel
HS-PDSCH	High-Speed Physical Downlink Shared Channel
HS-SCCH	High-Speed Shared Control Channel
HSUPA	High-Speed Uplink Packet Access
HW	Hardware
I	In-phase element of the modulation constellation
IMS	IP Multimedia Subsystem
IP	Internet Protocol
ITU	International Telecommunications Union
Iu	Interconnection point between the RNS and the Core Network
Iub	Interface between the RNC and the Node B
Iur	A logical interface between two RNCs
kbps	Kilobits per second
L1	Physical layer
L2	Data link layer
L3	Network layer
LLR	Log Likelihood Ratio
LMMSE	Linear Minimum Mean Squared Error
MAC	1. Medium Access Control. A control entity in the L2
	2. Multiply Accumulate Unit in any CPU
MAC-hs	High speed entity of Medium Access Control (MAC) protocol (TS 23.321)
MAP	Maximum a posteriori
MBMS	Multimedia Broadcast/Multicast Service
Mcps	Million chips per second
Mbps	Megabits per second
ME	Mobile Equipment

MICH	MBMS Notification Indicator Channel
MIMO	Multiple-input multiple-output
ms	Millisecond
NACK	Not Acknowledged
OCNS	Orthogonal Channel Noise Simulator
OFDM	Orthogonal Frequency-Division Multiplexing
OVSF	Orthogonal Variable Spreading Factor
P-CCPCH	Primary Common Control Physical Channel
PCH	Paging Channel
PDCP	Packet Data Convergence Protocol
pdf	Probability density function
PICH	Paging Indication Channel
PSPCH	Physical Downlink Packet Channel
PDSCH	Physical Downlink Shared Channel
PRACH	Physical Random Access Channel
Q	Quadrature-phase of the modulation constellation
QPSK	Quadrature Phase Shift Keying
RACH	Random Access Channel
RLC	Radio Link Control
RNC	Radio Network Controller
RRC	Radio Resource Control
SC-FDMA	Single Carrier Frequency Division Multiple Access
S-CCPCH	Secondary Common Control Physical Channel
SCH	Synchronization Channel
SF	Spreading Factor
SHO	Soft Handover
SIM	Subscriber Identity Module
SIR	Signal-to-Interference Ratio

TCH	Traffic Channel
TDD	Time Division Duplex
TFCI	Transport Format Combination Indicator
TFI	Transport Format Indicator
TTI	Transmission Time Interval. In case of 3GPP system TTI may be 2 ms (HSDPA), 10 ms, 20 ms, 40 ms or 80 ms
U-Plane	User Plane
UE	User Equipment (i.e. mobile phone or other device that is used to access the radio network)
UICC	UMTS Integrated Circuit Card
UMTS	Universal Mobile Telecommunications System
USIM	UMTS Subscriber Identity Module
UTRAN	UMTS Terrestrial Radio Access Network
Uu	The Radio interface between UTRAN and the User Equipment
WCDMA	Wide-band Code Division Multiple Access
WiMAX	Worldwide Interoperability for Microwave Access
WLAN	Wireless Local Area Network

LIST OF SYMBOLS

A	Amplitude of a signal
$\overline{A}$	Estimated amplitude of a signal
a	Smallest axis position of a symbol in the 64-QAM constellation
b_i	ith demodulated bit
$d(s,x)$	Euclidean distance between s and s
G	Geometry, calculated as $\mathrm{I_{or}}\,/\,\mathrm{I_{oc}}$
$\mathrm{I_{oc}}$	The power spectral density of a noise source as measured at the UE antenna connector.
$\mathrm{I_{or}}$	The total transmit power spectral density of the downlink signal at the BTS antenna connector.
i	1. Imaginary unit
	2. Index number
K	Number of estimation channels
k	Estimation channel index
N	Length of the estimation period
n	Estimation period index
P	Power of a signal
P_i	Power of channel i
$\overline{P}$	Estimated power of a signal
S_i	Partition of the 64-QAM constellation indicating that the ith bit is 0
$\overline{S_i}$	Partition of the 64-QAM constellation indicating that the ith bit is 1
s	Symbol belonging to either partition S_i or $\overline{S_i}$
s_i	ith demodulated soft bit
Thr	Demodulation threshold for the 64-QAM constellation
x	Incoming symbol to be demodulated

x_I	In-phase element of x
x_Q	Quadrature-phase element of x
μ	Mean
σ^2	Variance

x_I In-phase element of x

1. INTRODUCTION

1.1 History of mobile data transfer

Mobile data transfer has evolved at a very fast pace for the past 15 years. In 1990, the earliest digital mobile data transfer was achieved in Europe with the Global System for Mobile Communication (GSM), a second generation mobile technology (2G). GSM phones were designed to carry voice at a speed of 13 kbps on traffic channels (TCH). Although the TCH was designed for voice traffic, it could also be used to transfer data at speeds of 0.3 – 9.6 kbps.

In practice it soon became apparent that this data rate was too slow for most practical applications. Although third generation mobile technologies (3G) were already being specified, several improvements were made to increase data rates in GSM. Those improvements, published annually between 1997 and 1999, are referred to as GSM Phase 2+. The following improvements allowed much faster bit rates to be achieved: High-Speed Circuit Switched Data (HSCSD), General Packet Radio Service (GPRS) and Enhanced Data Rate for GSM evolution (EDGE).

HSCSD improved throughput by using different coding methods and multiple time slots, allowing a throughput of up to 115 kbps. Data rates of 171.2 kbps could theoretically be reached with GPRS, which introduced a packet-switched GSM (as opposed to circuit-switched). As a final improvement to GSM, EDGE allowed speeds up to 473.6 kbps with a new modulation type, 8 phase shift keying (8PSK).

The first 3G Universal Mobile Telecommunications System (UMTS) networks using Wide-band Code Division Multiple Access (WCDMA) were specified by the 3rd Generation Partnership Project (3GPP) in 1999. 3GPP is a standardization project formed by telecommunications groups from Europe, Japan, Korea, China and the United States. Generally called Release '99, the first UMTS networks used new modulation types and spreading codes to increase speeds theoretically up to 2 Mbps. First commercial UMTS networks were taken into use in 2001.

3GPP has since then released several additions to UMTS, increasing data rates and introducing new services. In 2002 Release 5 introduced high-speed downlink packet access (HSDPA). Using adaptive coding, fast retransmissions, fast packet scheduling, multi-code operation and 16-QAM modulation HSDPA could theoretically deliver a throughput of 14.4 Mbps with low latency in downlink. The first commercial HSDPA networks were taken into use in 2007.

The biggest problem with HSDPA is that uplink data rates remain the same as in Release '99. In 3GPP Release 6 high-speed uplink packet access (HSUPA) was introduced to counter this problem. It used the same techniques in uplink an HSDPA used in downlink, allowing uplink speeds of up to 5 Mbps. The first HSUPA networks were also taken into use in 2007. Release 6 also introduced WLAN integration, allowing speeds of up to 54 Mbps when WLAN is available.

Currently in 2007, 3GPP has almost finished Release 7. Among other things, it will present two improvements to HSDPA: Multiple-input multiple-output connections (MIMO) and 64 Quadrature Amplitude Modulation (64-QAM). MIMO is based on the principle of two transmitters and two receivers transmitting two separate data streams over the same radio channel, potentially doubling the maximum bit rate to 28.8 Mbps. 64-QAM allows more data to be carried on the same bandwidth, increasing the potential throughput to 21.6 Mbps. Release 7 also improves WLAN support, allowing data transfer rates beyond 100 Mbps.

Release 8 is currently planned for a 2009 release. Among other things it will allow MIMO and 64-QAM to be used simultaneously, increasing the maximum theoretical throughput to 43.2 Mbps. Another project within 3GPP is called long term evolution (LTE). Preliminary plans include increasing bandwidth up to 20 MHz and using Orthogonal Frequency-Division Multiplexing (OFDM) to increase downlink to 100 Mbps and uplink to 50 Mbps.

Then again fourth generation telecommunications technologies are already being designed. With some estimates predicting that we will see 4G networks by 2015, it is clear that most things about 4G are still speculation. A general way of describing 4G is the All-IP (Internet Protocol) model. All services would be carried over an integrated network, offering speeds of up to 1 Gbps in good conditions. The general principle is that all services would be available anywhere. Many access technologies have been proposed, among them OFDM, Single Carrier Frequency Division Multiple Access (SC-FDMA) and Multi-carrier code division multiple access (MC-CDMA). In any case, it seems that mobile data rates will continue to rise.

1.2 Objective of this Thesis

This thesis will focus on the new 64-QAM modulation type used by HSDPA in Release 7. 64-QAM allows more bits to be transmitted over the air interface without increasing the bandwidth or decreasing the number of users, allowing an even higher spectral efficiency and peak data rates than Release 5 HSDPA. Studies such as [Eri06a] and [Eri06b] have shown a substantial increase in average data rates when using 64-QAM. Higher data rates allow for example higher quality video

telephony and other multimedia services. The downside is that 64-QAM is much more sensitive to errors than 16-QAM, the highest modulation scheme used in Release 5 HSDPA. The signal-to-noise ratio required by 64-QAM is approximately 6 dB higher than with 16-QAM [Hol07].

To support 64-QAM mobile phone modems will have to be redesigned. Memory will have to be increased to support the higher bit rates and new algorithms will have to be designed to correctly receive the 64-QAM modulated signal. Accurate amplitude estimation is important so that the modulated symbols can be separated from each other. A demodulation scheme that reliably decodes the bits is also needed.

This thesis aims to find which algorithms allow best bit rates with a Release 7 HSDPA mobile phone using 64-QAM. Since Release 7 equipment will not be available for some years, a physical layer HSDPA simulator will be used to reach the objective.

1.3 Structure of the Thesis

The rest of this thesis is divided in the following way: Chapter 2 will give an introduction to UMTS. Chapter 3 will explain HSDPA in more detail, focusing on the physical layer. In chapter 4, the challenges related to 64-QAM will be explained and different algorithms presented. Chapter 5 will explain the simulation setup and present the results. Chapter 6 will offer a summary and conclusions.

2. UMTS

2.1 Overview

This chapter gives a short introduction to UMTS architecture and functionality focusing on the physical layer. Although this thesis focuses on HSDPA, some basic knowledge about UMTS and WCDMA is needed to understand the following chapters. All information in this chapter is taken from [Hol07] unless otherwise mentioned.

2.2 Network architecture
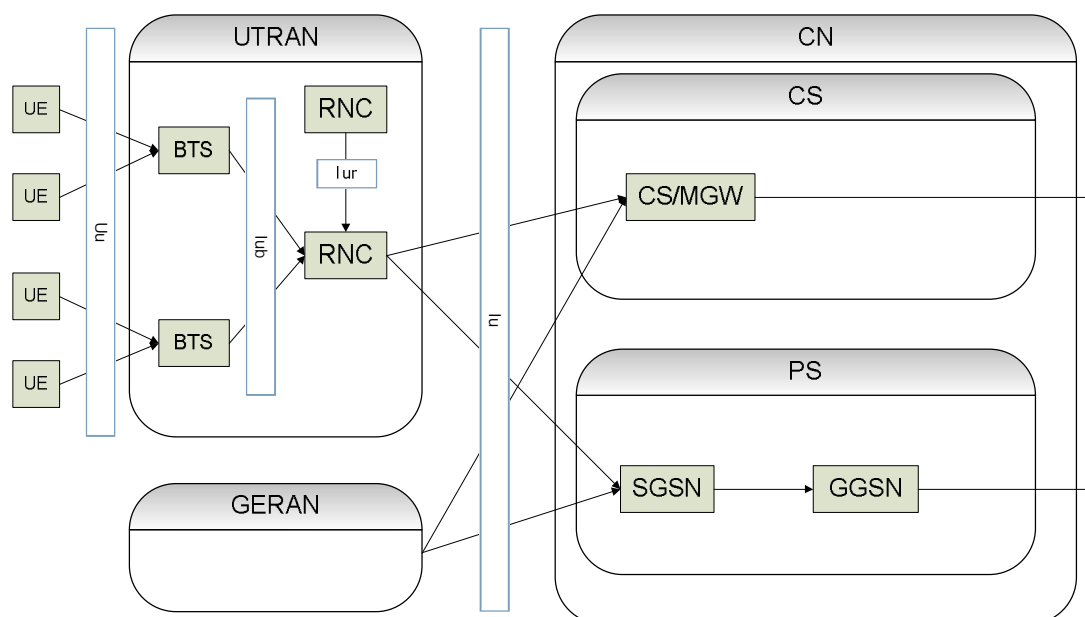
Figure 2-1: UMTS network architecture

The general UMTS network architecture can be seen in Figure 2-1. It follows the same principle as 2G networks but completely changes the air interface. On the highest level the network is divided to the following logical components: the user equipment (UE), the UMTS terrestrial radio access network (UTRAN), the core network (CN) and the interfaces between them. UE is simply the means the device the user uses to access the network, consisting of mobile equipment (ME) and UMTS subscriber identity module (USIM). ME is simply the cell phone or some other mobile device like a laptop. USIM is an application for identifying the user and giving authentication for access to the network. USIM is usually contained on an UMTS integrated circuit card (UICC), generally called a SIM card. In addition to the network elements, the interfaces between them have also been standardized (*Uu, Iub, Iur*

and *Iu* in the figure). The interfaces are extremely important so that products from different manufacturers can function together.

UTRAN allows connectivity between the ME to the CN. It contains base transceiver stations (BTS), radio network controllers (RNC) and the interfaces between them. The BTS, also called Node B, converts the data flow from the ME to the RNC. As data rates increase and smaller delays are needed the BTS also takes care of some radio resource management. The radio network controller (RNC) controls the resources of every BTS connected to it. The RNC is also the link between the rest of UTRAN and the CN.

The core network is responsible for switching and routing calls and data connections to external networks. It is divided into two parts: the circuit-switched (CS) network and the packet-switched (PS) networks. CN is compatible with both 2G and 3G networks, which allows both old and new phones to be connected to the same core network. Therefore in Figure 2-1 the GSM EDGE radio access network (GERAN) is also connected to the CN.

2.3 Radio protocol architecture
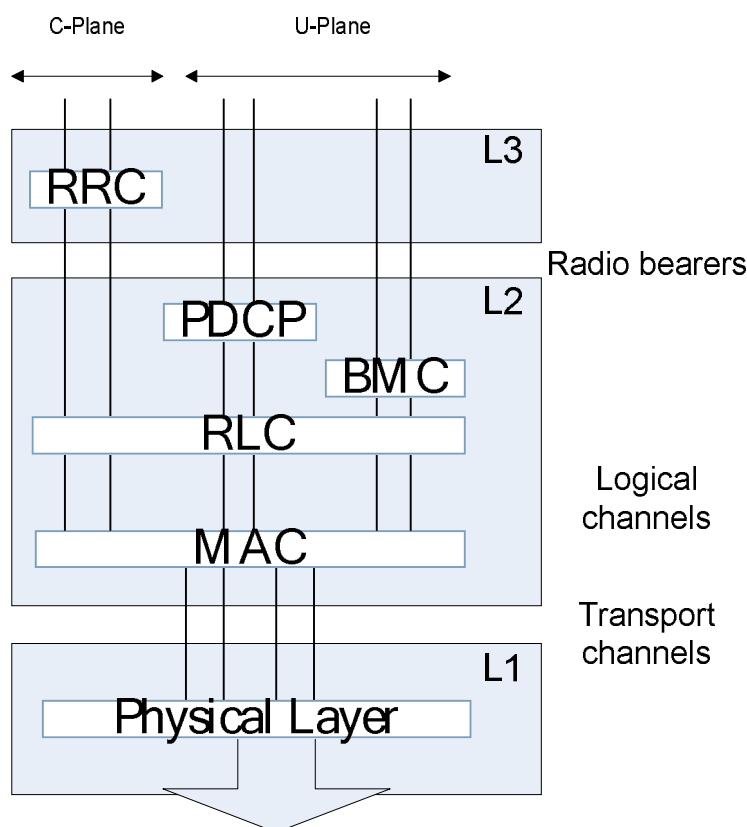
Figure 2-2: UTRAN radio interference protocol architecture

The radio interface (Uu) is the interface between the mobile station and the base station. Radio protocol architectures are needed to set up, reconfigure and release radio bearer services. The radio interface protocol architecture is divided into three layers:

- Physical layer (L1)

- Data link layer (L2)

- Network Layer (L3)

The architecture can be seen in Figure 2-2. L2 is divided into several sublayers. In the control plane, L2 consists of Medium Access Control (MAC) and Radio Link Control. In the user plane, there are the additional layers of Packet Data Convergence Protocol (PDCP) and Broadcast/Multicast Control Protocol (BMC). L3 contains one sublayer, Radio Resource Control (RRC) in the c-plane.

The physical layer offers data transport services to the MAC layer in the form of transport channels. Transport channels define how and what is transported over the air interface. MAC in turn offers services to RLC in the form of logical channels. Logical channels define what type of data is transmitted. RLC offers services to the upper layers with radio bearer channels. These services define how data is handled, for example are retransmissions needed.

The rest of this chapter focuses on the physical layer because it is the only layer relevant to the research problem in this thesis. Detailed information about the other layers can be found in e.g. [Hol07] and [3GPP_301]. Note that the physical channel will be described mostly according to 3GPP Release '99. Additions brought by HSDPA will be discussed in more detail in chapter 3.

2.4 WCDMA

The technology used by UTRAN to transport information over the air interface is wide-band code division multiple access (WCDMA). It is based on spreading the information over a large bandwidth. This is done by multiplying the outgoing signal with a spreading signal with a much higher bit rate than the data signal. This allows much higher spectral efficiency and bit rates than the interface used in GERAN networks. Spectral efficiency measures how large bit rates can be achieved with a given bandwidth.

WCDMA can support both time division duplex (TDD) and frequency division duplex (FDD). These two modes go under the names 3GPP TDD and 3GPP FDD. Since in Europe TDD is very rarely used in mobile telephony, it will not be covered further in

this thesis. For the rest of this thesis the abbreviation WCDMA is used to refer to 3GPP FDD.

2.4.1 Spreading

It is important to understand the difference between the data signal and the spreading signal. The data signal is made up of data bits and it contains the information to be sent over the air interface. The data bits are modulated into symbols before being transmitted. The spreading signal is a semi-random sequence derived from CDMA spreading codes. The bits of the spreading signal are called chips, and in WCDMA the chip rate has been set to 3.84 million of chips per second (Mcps). Also to separate data bits from spreading bits, data bits will be called *symbols* and spreading bits *chips* from now on.

In general a data signal consists of zeros and ones, but in this section symbols have values '-1' and '1'. This is done to allow convenient multiplying. The data and spreading signals are multiplied to spread the data signal to a wider bandwidth. The ratio of the WCDMA chip rate to the data rate is called the spreading factor (SF). The SF indicates how much the bandwidth widens or in other words with how many chips is each data symbol multiplied with. For example if the data rate is 480 kbps, the spreading factor is 8:

$$SF = \frac{3.84Mcps}{480kbps} = 8\left[\frac{chips}{bit}\right]$$

(1)

Spreading factors can vary from 2 to 512 in WCDMA.

If the spreading code is known at the receiver, the original signal can be decoded perfectly by correlating it again with the spreading signal. An example in Figure 2-3 illustrates this. Each data symbol is multiplied by a sequence of eight chips, so the spreading factor is also eight. It can be seen that the spread signal approximately follows the same pattern as the spreading signal.

Of course because of noise and interference the symbols cannot always be decoded perfectly. That is why a correlation receiver, generally called a despreader, is used. The despreader integrates all chips belonging to one symbol, as can be seen on the lowest row in Figure 2-3. The result of this integration at the symbol border is used as the symbol value. The correlation receiver also allows the correct signal to be received. Figure 2-4 illustrates what happens when the spread signal is despread with the wrong spreading code. There are no clear data symbols and the despreader integral at the symbol border stays near zero.
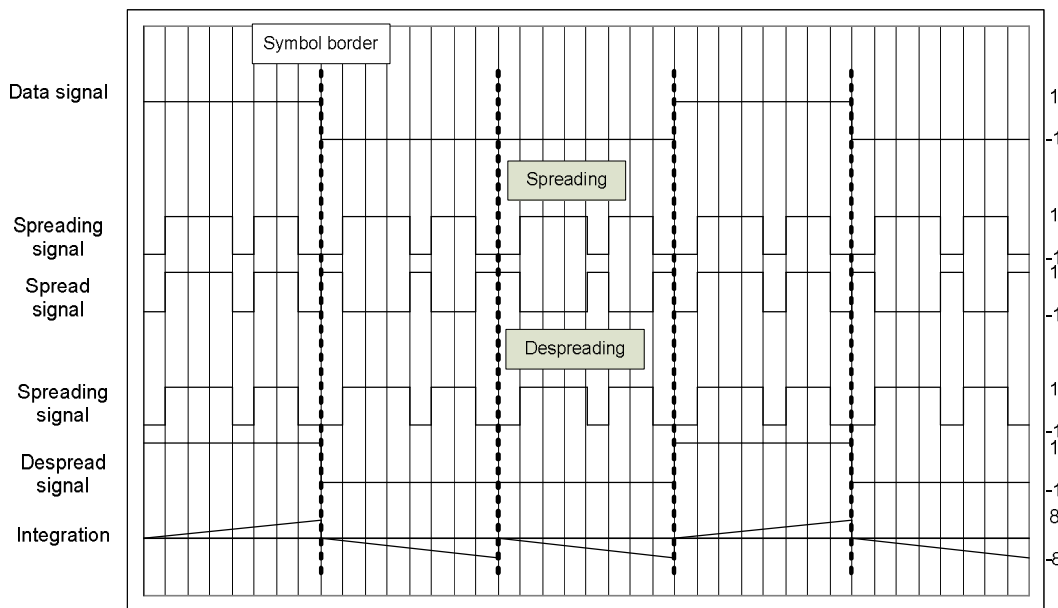
Figure 2-3: Example of spreading and despreading
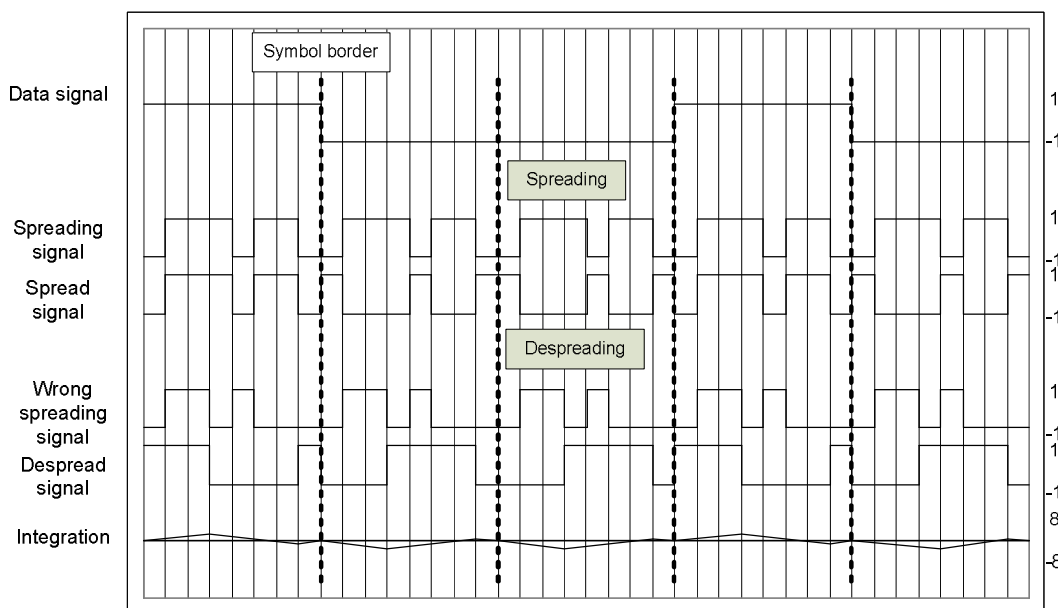
Figure 2-4: Example of despreading with the wrong despreading code

Because of the integration, the amplitude of the signal increases on average by the spreading factor. On the other hand, if the signal is spread with the wrong code, the amplitude doesn't increase at all. This property of WCDMA is called processing gain. Due to this effect the wideband signal can actually be weaker than noise and the correlation receiver can still receive the signal correctly.

Since the spreading factor is directly proportional to the processing gain, it can be modified based on channel conditions. If the used spreading factor is high, the signal can still be received in noisy conditions. Respectively the data rate is lower,

because more chips are needed to transmit one data symbol. Variable spreading factor is not the only way to adapt to changing channel conditions, power control explained in 2.4.3 is another method.

2.4.1.1 Spreading codes

This section explains how the pseudo-random spreading code is generated and applied. The spreading code is actually a combination of two codes: the channelisation code and the scrambling code. The relationship between the two can be seen in Figure 2-5. The figure simplifies the process somewhat, in reality the codes are usually applied to modulated symbols. This will be explained in more detail in section 2.5.3.
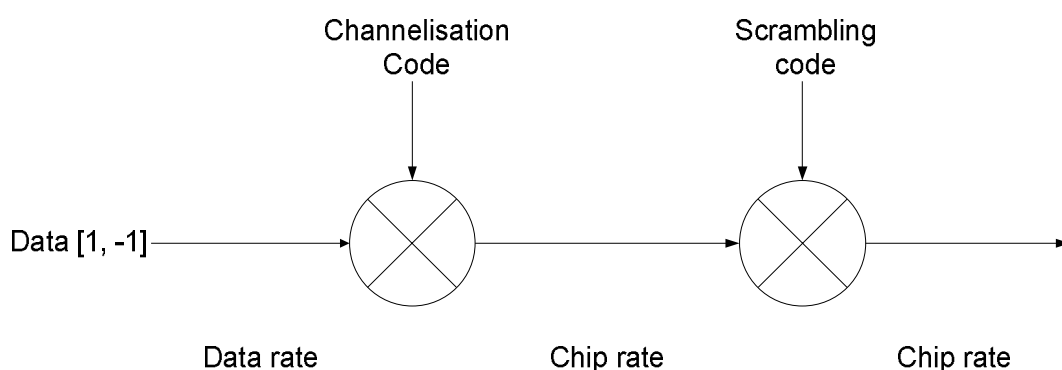
Figure 2-5: Spreading process

The channelisation code spreads the signal to the wider bandwidth, and has a chip rate of 3.84 Mcps. It is also used to separate signals from a single source from each other. For example a mobile terminal can signal multiple data and control channels simultaneously.

The codes are generated based on the orthogonal variable spreading factor (OVSF) [Ada97] technique. The principle of OVSF and an example of a short code tree can be seen in Figure 2-6. The size of the tree depends on the spreading factor. Since different channels can use different spreading factors, there are simple rules for which channelisation codes can be used. If a code is used, none of the codes following or preceding it in the code tree can be used. So if code (1, 1) is used, codes (1), (1, 1, 1, 1) and (1, 1, -1, -1) cannot be used (see Figure 2-6).

(1, 1, 1, 1)

(1, 1)

(c, c)

(1, 1, -1, -1)

(c)

(1)

(c, -c)

(1, -1, 1, -1)

(1, -1)

(1, -1, -1, 1)
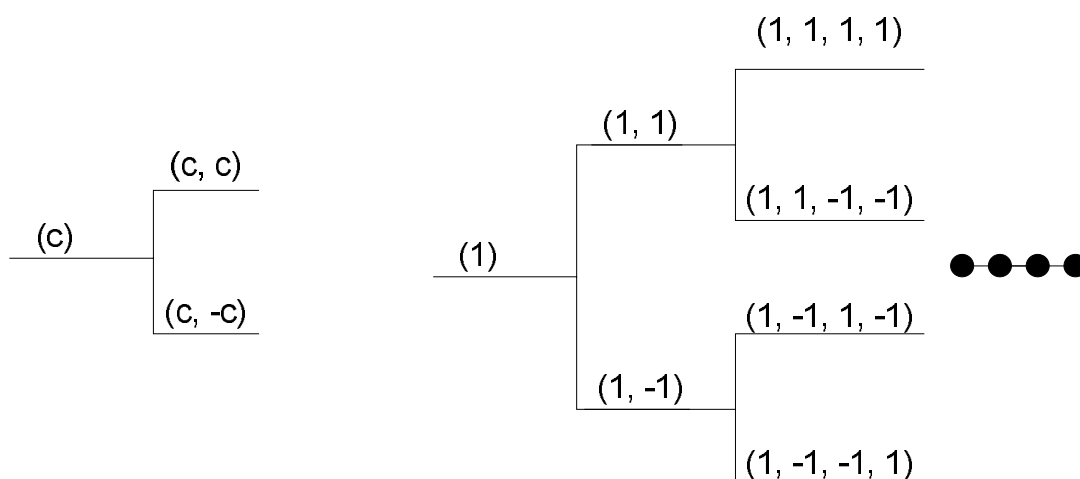
Figure 2-6: OVSF channelisation principle and the beginning of a code tree

Where channelisation codes spread the signal to a wider bandwidth and distinguish channels from each other, scrambling codes are used to separate terminals in the uplink (signals sent from UE to BTS) and base stations in the downlink (signals sent from BTS to UE) from each other. Scrambling codes do not change the bandwidth of the signal. Because of the scrambling codes, separate cell phones and base stations can use the same channelisation code tree independent of each other. Code management is needed so that different terminals in the same coverage area do not use the same scrambling code. Because of the scrambling codes base stations next to each other can use the same frequency band, allowing WCDMA to utilize the available bandwidth very efficiently.

There are many ways to generate scrambling codes, although in WCDMA only two different methods are used: short S(2) codes and long Gold codes. Both have been specified in [3GPP_213].

2.4.2 Rake receiver

A common problem in telecommunications is multipath propagation. The transmitted signal reflects and diffracts from large objects like buildings and mountains. The result is that several instances of the same signal are received at the mobile station. These signals have different phase and power because of energy lost to reflection and longer propagation length. Also if two signal instances arrive at the same time but have opposite phase, they cancel each other out.

WCDMA uses e.g. Rake receivers to counter multipath problems. A Rake receiver is made up of multiple correlation receivers called Rake fingers. Each finger is allocated to the time instant that a new multipath signal arrives. When all fingers

have collected the signal, the phases are normalized and the signals are combined to maximize the utilized transmission power.

2.4.3 Power Control

One important property of WCDMA is fast power control. It is used both in uplink and downlink. In uplink power control is used to combat the so called *near-far problem*. In a situation where one UE is just next to a BTS and another is very far, the signals from the near UE can drown the signals from the other UE.

The solution is to normalize the transmission power of every UE. In WCDMA the BTS calculates the Signal-to-Interference Ratio (SIR) of every UE 1500 times a second. The base station has a certain target SIR, and if a measured SIR is too high a signal is sent to the UE to lower its transmission power. If the received SIR is too low the UE is instructed to increase transmission power. Because of the high frequency of the measurements, power control in WCDMA is called fast power control.

In the downlink there is no near-far problem because all the mobile stations receive the same signal sent by the BTS. Because all signals originate from the same place, the scrambling codes remain orthogonal and every UE can easily separate the correct signals. Downlink power will still have to be controlled, because too large power causes interference to neighbouring base stations. Every UE measures the SIR of the downlink signal, and requests the BS to increase or decrease transmission power if needed.

2.4.4 Soft Handover

The coverage area of a BTS is divided into multiple sectors. Soft handover (SHO) occurs when a mobile station is in the coverage area of multiple sectors. Where in 2G networks the connection trough the old sector is cut before the new one is established, in WCDMA the UE is connected through all nearby sectors simultaneously. The sectors can belong to the same base station, multiple base stations or even multiple radio network controllers. If all the sectors belong to the same BTS, SHO is called softer handover.

There are several benefits of a soft handover. First of all it increases reliability, because if the call setup through the new sector fails, the old connection is still active. In 2G networks the call would have been lost. SHO also removes the ping-pong effect, which occurs when a UE is moving on the edge of two sectors. This effect means that the call is continuously being reconnected through the other

sector. Lastly it makes power control more effective, because when moving to the edge of a new sector the new BTS can also contribute to power control.

In downlink SHO works pretty much the same way as multipath reception. Different Rake fingers are allocated to the different scrambling codes of the sectors and the signal is combined. In uplink things vary somewhat. In softer handover things go the same as in downlink: the Rake receiver in the BTS combines the multiple signals from the UE. However if the ME is connected to multiple base stations, all signals are sent to the RNC. There the reliability of all received radio frames is compared, and the best one is selected.

2.5 Physical layer

This section describes the physical layer mentioned in section 2.3. It is discussed in more detail than other aspects of WCDMA because it is the most relevant to this thesis: the demodulation of 64-QAM discussed in Chapter 4 is a physical layer task.

2.5.1 Transport channels

The MAC layer sends transport blocks to the physical layer for transport over the air interface. Transport channels are a service offered to the MAC layer by the physical layer. Transport channels define how and with what characteristics is data transported over the air interface. Transport channels are mapped onto physical channels, which will be described in section 2.5.2.

Each transport channel is accompanied by a Transport Format Indicator (TFI). TFI indicates the type of the transport channel and other characteristics like transmission rate. After the transport channels are mapped onto a physical channel, the physical channel is accompanied by a Transport Format Combination Indicator (TFCI). TFCI is a combination of the TFIs of the transport channels mapped on to the physical channel, and informs which transport channels are active in the frame.

Transport channels are divided into dedicated transport channels and common transport channels. Dedicated channels transport data to only one UE, and they are separable by a code and frequency. Common channels transport data to a group of users in the same sector.

2.5.1.1 Dedicated transport channel

There is only one dedicated transport channel in Release '99, called the dedicated channel (DCH). It can be used to transport all information from the higher layers to the whole sector in both uplink and downlink. Because DCH is used to transport different kinds of data (for example speech frames, control information etc.), the data rate of the channel can be varied every 10 ms (one frame).

Release 6 introduced a new dedicated transport channel: the enhanced dedicated channel (E-DCH). It provides high speeds (5.8 Mbps) in the uplink to be used with HSUPA. HSUPA will not be covered further in this thesis.

2.5.1.2 Common transport channels

The broadcast channel (BCH) is a downlink channel transmitted to every UE in the sector and it contains system- or sector-specific information like the type of transmit diversity methods and random access codes. BCH is transmitted with high power so that it can reach every user in the sector. It also has a low data rate that every UE can decode it. The BCH transmission sent by the BTS must be received and decoded by the UE before the sector's services can be used. The BCH is mapped to the primary common control physical channel (P-CCPCH).

The forward access channel (FACH) is a downlink channel used to send control information to the UE. Like with the BCH the information is transmitted to the entire sector, but there can be multiple FACH channels active in a sector. That way high-end mobile equipment can receive better data rates than low-end ones by receiving multiple FACH channels. The FACH is mapped to the secondary common control physical channel (S-CCPCH).

The paging channel (PCH) is a downlink channel used to relay paging information to the UE, for example a notice that a voice call is incoming. The PCH can be transmitted to multiple sectors simultaneously, if there is uncertainty where the UE is located. The PCH is designed so that the UE can continuously monitor for paging messages with low power consumption. The channel contains a paging message to indicate which UE the signal is meant for. The PCH is also mapped to the S-CCPCH.

The random access channel (RACH) is an uplink channel used to transport control information from the UE to the BTS. As BCH, RACH transmissions must work from the entire sector coverage area so the transmission power is high and the data rate low. The RACH is mapped to the physical random access channel (PRACH).

The high-speed downlink shared channel (HS-DSCH) is a downlink channel used to transport HSDPA data at high data rates and it will be described in chapter 3.

2.5.2 Physical channels

The data contained in the transport channels is mapped on to physical channels for transport over the air interface. The mappings can be seen in Figure 2-7. Physical channels are separated by carrier frequency, scrambling code and channelisation code. As transport channels, physical channels are also divided into shared and

dedicated channels. It is possible for one physical control channel and at least one physical data channel to be multiplexed together to form a coded composite transport channel (CCTrCh).

BCH ———————————— PCCPCH

FACH ————————————— SCCPCH

PCH

RACH ———————————— PRACH

DCH ———————————— DPDCH

DPCCH

F-DPCH

E-DCH ———————————— E-DPDCH

E-DPCCH

HS-DSCH ———————————— HS-DPSCH
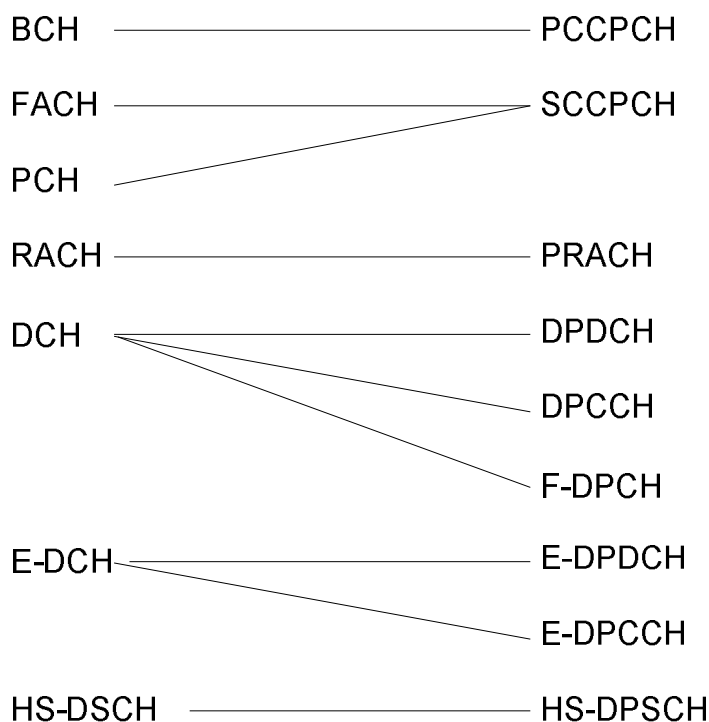
Figure 2-7 Transport channel mappings to physical channels

Duration of a channel is specified by its start and stop time. There are a few standard durations generally used in specifications. A radio frame is a processing period 10 ms long (38400 chips). The frame is further divided into 15 slots, each with a length of 2560 chips. A third generally used duration is one sub-frame, which has a length of 3 slots (7680 chips). The radio frame structure can be seen in Figure 2-8.

2560 chips (1 slot)				2 ms (1 sub-frame)			

1	2	3	...											15

10 ms (1 frame)
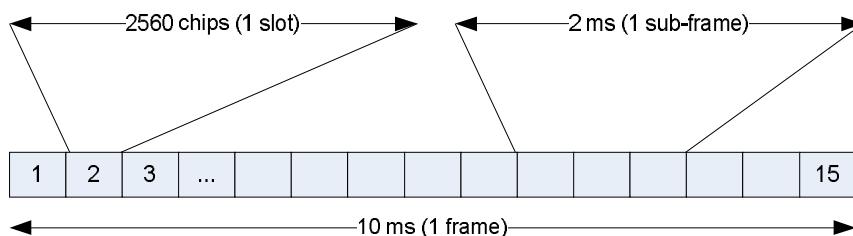
Figure 2-8: Radio frame structure

2.5.2.1 Dedicated Physical Channels

Dedicated physical channels are channels transmitted to only one destination. The DCH is mapped to the dedicated physical channel (DPCH). There are two kinds of DPCH channels: the dedicated physical data channel (DPDCH) and the dedicated physical control channel (DPCCH). The DPDCH carries the actual user data and the DPCCH carries control data needed by the channel. The channels are used both in the uplink and downlink, but they have some differences.

The biggest difference is that in the uplink the DPCCH and DPDCH are I/Q multiplexed and in the downlink QPSK-modulated and time-multiplexed. This is explained in section 2.5.3. The data contained in the DPCCH is also a little different depending on the transmission direction. In the downlink the channel contains feedback information, the pilot signal and power control commands. In the uplink the channel also contains transport format information.

There also exist modified versions of the channels. The enhanced DPDCH (E-DPDCH) and the enhanced DPCCH (E-DPCCH) are used to carry the E-DCH channel in the uplink. The fractional dedicated physical channel (F-DPCH) is a stripped down version of downlink DPCCH that carries only power control information.

The final dedicated uplink physical channel is the high-speed dedicated physical control channel (HS-DPCCH). It carries HSDPA control information and is described in chapter 3. All dedicated uplink channels (DPCCH, DPDCH, E-DPDCH, E-DPCCH and HS-DPCCH) are I/Q multiplexed together. There exist also two dedicated downlink physical channels that are required by HSUPA: the E-DCH relative grant channel (E-RGCH) and the E-DCH hybrid ARQ indicator channel (E-HICH).

2.5.2.2 Common Physical Channels

Common physical channels transport information on the common transport channels to all UE in range. The different mappings can be seen in Figure 2-7 and they are also mentioned in section 2.5.1.2. The specific operation of common physical channels is not relevant to this thesis so they are not covered here in more detail. For more detailed information see e.g. [Hol07] and [3GPP_211].

In addition to the listed physical channels there exist common physical channels for signalling purposes. These channels have no transport channels mapped to them but they are still necessary for transmission purposes.

- The synchronization channel (SCH) is used by UE to find sectors and time-synchronize with them.

- The common pilot channel (CPICH) transmits a pre-defined symbol sequence to help terminals with channel estimation.

- The collision detection/channel assignment indicator channel (CD/CA-ICH) is used to carry collision detection indicators (CDI) and channel assignment indicators (CAI).

- The paging indication channel (PICH) is used to inform UE about incoming calls before establishing a PCH connection.

- The acquisition indication channel (AICH) is used to inform UE that the network successfully received a RACH channel.

- The MBMS indicator channel (MICH) is needed for multimedia broadcast / multicast service (MBMS).

- The E-DCH absolute grant channel (E-AGCH) is needed by HSUPA.

- The high-speed shared control channel (HS-SCCH) is used to transport HSDPA control data, and is explained in chapter 3.

2.5.3 Data transmission

This section describes how user data (a transport block from a higher layer) is transformed into a physical signal transmitted over the air interface [3GPP_212]. Transmission is slightly different between uplink and downlink, so they will be explained separately. The main principle is same for both cases: the received bits are first coded to the transport channel. The resulting transport channel(s) are then mapped to the appropriate physical channels and the channels are modulated. The data symbols of the physical channels are then spread with the spreading and scrambling codes and finally transmitted as root-raised cosine (RRC) pulses. This chain can be seen in Figure 2-9.

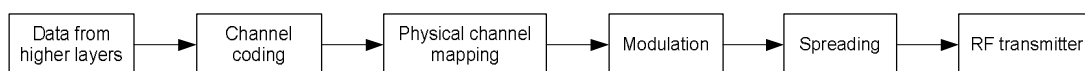| Data from higher layers | → | Channel coding | → | Physical channel mapping | → | Modulation | → | Spreading | → | RF transmitter |

Figure 2-9: Data transmission chain

2.5.3.1 Uplink

The uplink channel coding and multiplexing chain can be seen in Figure 2-10. First, a cyclic redundancy check (CRC) is used so that error checking can be performed at the receiver. Next the transport block is either concatenated or segmented into coding blocks, depending on the size of the block. The code blocks are then coded

with either convolutional coding or turbo coding, depending on the transport channel type.

There are three different coding methods defined for Release '99. Half-rate and 1/3 –rate convolutional coding are used for low data rates such as speech. 1/3 –rate turbo coding is used for higher data rates, it has been estimated that if over 300 bits are transmitted in one TTI turbo coding is better.
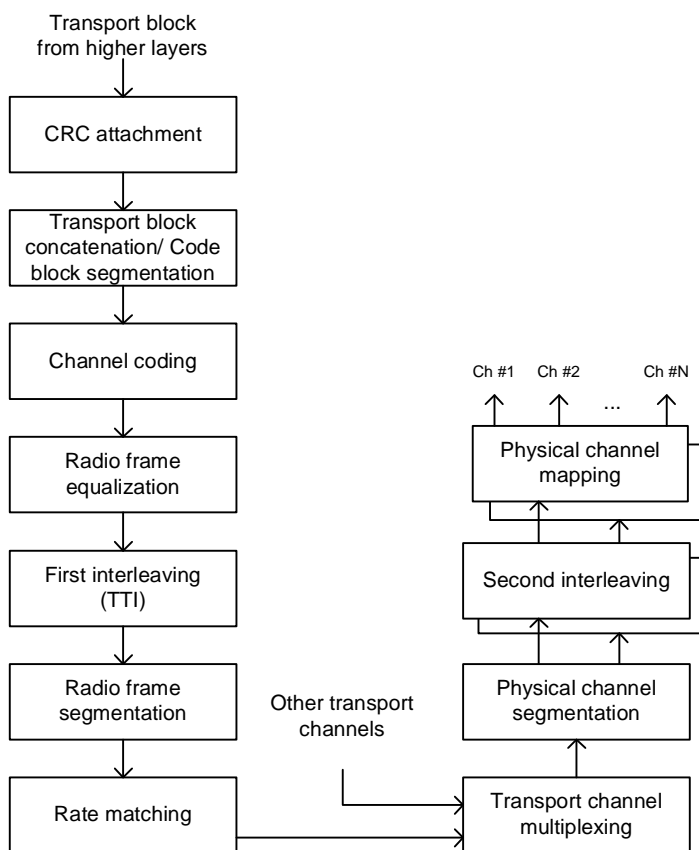
Figure 2-10: Uplink channel coding and multiplexing

The next two operations depend on the transmission time interval (TTI), which indicates how often a new transport block arrives from higher layers. In Release '99 possible values for TTI are 10 ms, 20 ms, 40 ms and 80 ms. If a larger TTI than 10 ms is used, the coded blocks are then equalized by padding bits so that they can be evenly divided into 10 ms frames. After the equalization the blocks are interleaved into the radio frames. So for example if the TTI is 80, the coded block is divided into eight equal sized segments and interleaved into consecutive radio frames.

Rate matching makes sure that all bit capacity on the radio frame is used. If the interleaved data is less than the frame capacity, repetition is usually used to fill the frame. Note that rate matching must also take into account data coming from other transport channels.

If more than one transport channel is being mapped to the physical channel, the transport channels are multiplexed together. If multiple physical channels are used, the multiplexed transport channels are segmented to the appropriate channels. Finally each physical channel goes through second interleaving, in which the 10 ms frames are interleaved into 30 columns and inter-column permutation is used. This permutation is used to counter bursty transmission errors.

Next the data bits are mapped to the appropriate physical channels. In the uplink I/Q multiplexing, also called dual-channel QPSK, is used. When this modulation type is used the data flow is continuous even if there is no traffic on the data channel. This is good, because gaps in the transmissions cause audible interference to other devices.

In I/Q multiplexing both the actual data contained on the channel and the control information related to it are first separately BPSK-modulated. The control signal is then shifted by 90° and normalized to have the same power as the data channel. The two signals are then combined into one QPSK-modulated signal. BPSK and QPSK constellations can be seen in Figure 2-11.
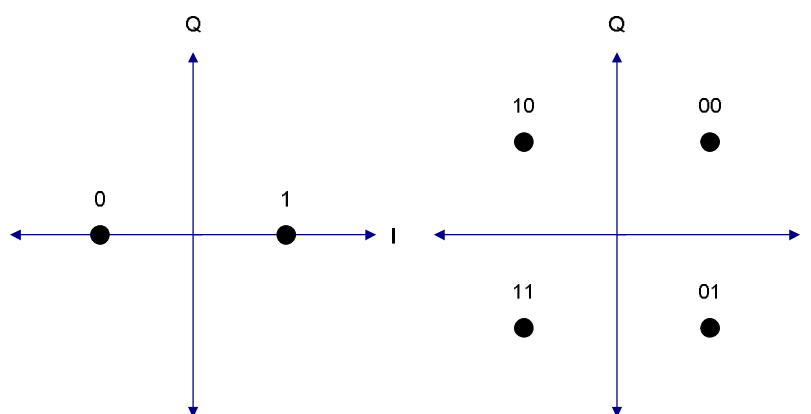
Figure 2-11: BPSK and QPSK constellations
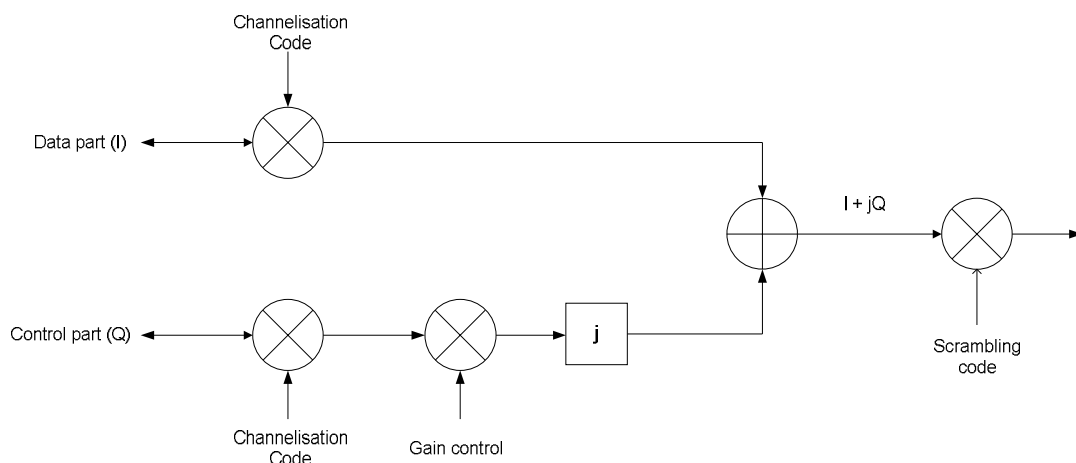
Figure 2-12: Spreading operation in the uplink

Channelisation and scrambling codes are applied before transmission. Different channelisation codes are used for the control and data channels, but the scrambling code is used after the two signals are combined. This complex-valued chip signal is then scrambled with a complex scrambling code. The relationship between channelisation and scrambling in I/Q multiplexing can be seen in Figure 2-12. The spread signal is then transmitted over the air as RRC-pulses.

2.5.3.2 Downlink
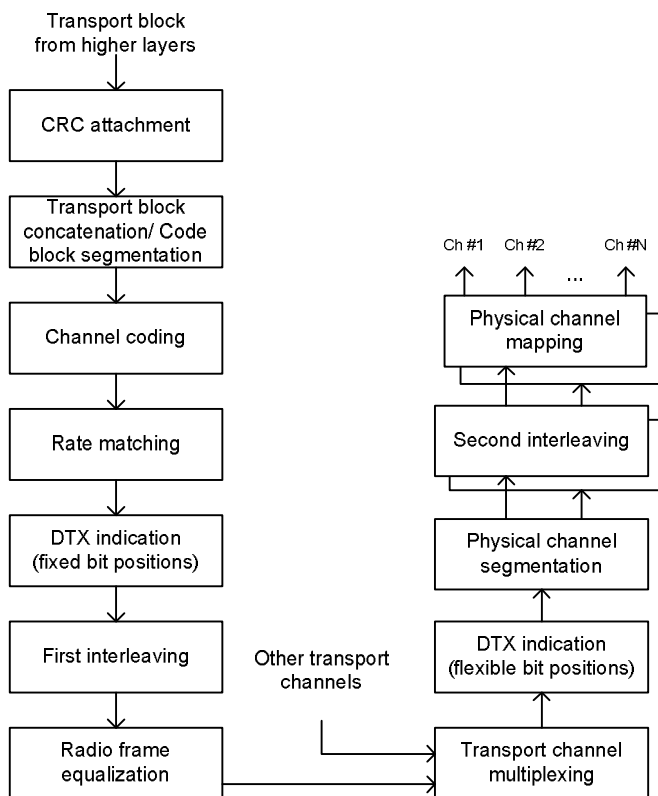
Figure 2-13: Downlink channel coding and multiplexing

Downlink data transmission is very similar to uplink, channel coding and multiplexing can be seen in Figure 2-13. In this phase the only differences are the order of the operations and one new operation: discontinuous transmission (DTX) indication.

DTX is a power saving method for when there is no data to be sent. In the uplink the transmitter is simply turned off to save power, but in the downlink this is not possible due to continuously transmitted common channels (like the BCH). It is however possible to inform the UE that there is no data incoming with the DTX indication, allowing the terminal to shut down its receiver for a time. In this method of DTX the indication bits are always in the same place in the transport channel. It is also possible to use flexible bit positions so that the free bits can be utilized by some other service. In that case the DTX indication bits are added after transport channel multiplexing.

A bigger difference between uplink and downlink comes in the modulation. Since in the downlink there are continuously transmitted common channels, there is no problem with gaps in transmission. Therefore instead of combining control and data channels, all channels are modulated with normal QPSK. That means two bits are modulated at a time from each channel. The mapping can be seen in Figure 2-11. The only exception is the HS-PDSCH channel used with HSDPA, which supports other modulation types. The channel will be described in chapter 3.

After the modulation the same channelisation code is used on both I- and Q-branches of the signal. The complex symbol is then scrambled as in the uplink. The downlink spreading operation can be seen in Figure 2-14. Data and control channels are time-multiplexed in the downlink, which means they are sent one after the other.
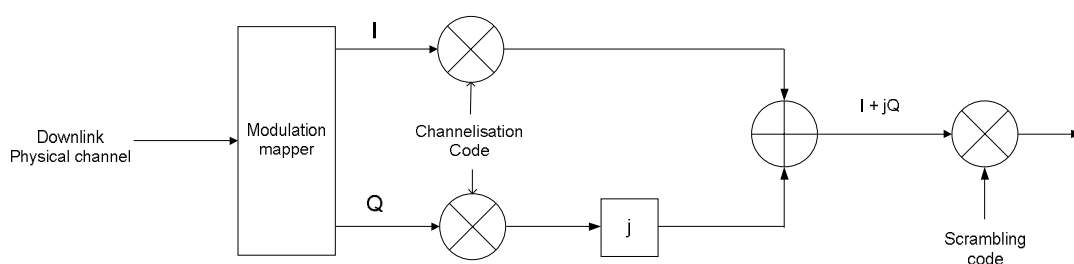

Figure 2-14: Spreading operation in the downlink

3. HSDPA

3.1 Overview

High-speed downlink packet access (HSDPA) is a 3G technology introduced in 3GPP Release 5. It was released in 2002 so that UMTS would be able to compete against new technologies like CDMA-2000 and WiMAX. The main benefit of HSDPA is that it can greatly increase throughput in WCDMA networks with very small changes to the network. All information in this chapter is taken from [Hol06] unless otherwise mentioned.

HSDPA introduced in Release 5 delivers considerably higher average user throughput than Release '99 and peak data rates of up to 14.4 Mbps in the downlink. This is achieved with fast physical layer retransmissions, transmission combining and fast link adaptation. New HSDPA features introduced in Release 7 allow data rates of 21.6 Mbps with higher-order modulation and 28.8 with Multiple-input multiple-output (MIMO).

3.2 New features

HSDPA aims to improve WCDMA throughput by very similar means to how EDGE improved GSM. HSDPA is based on four reforms:

- Adaptive modulation and coding (AMC)

- Hybrid automatic repeat request (HARQ)

- Fast packet scheduling

- Short (2 ms) transmission time interval (TTI)

In Release '99 three transport channels were used to transport user data: DCH, DSCH and FACH. HSDPA adds a new transport channel that puts the new HSDPA features to use: the high-speed downlink shared channel (HS-DSCH).

In Release '99 retransmission was used to improve reception accuracy. If a packet was not decoded properly in the UE, the same packet or a modified one was retransmitted from the RNC. This retransmission method is called automatic repeat request (ARQ). Because the packet is retransmitted from the RNC, ARQ causes quite a high latency. That is why in HSDPA introduces HARQ, which is basically an improved ARQ moved to the base station. The old packet is not discarded, but combined with the retransmitted packet to increase reception accuracy. Because the

packets are retransmitted from the BTS HARQ is faster than ARQ, but the combining requires extra buffer for the BS and the UE.

In Release '99 the BS continuously monitors the channel quality at the UE and adapts the power and spreading factor of the channel to ensure best throughput. In HSDPA downlink fast power control and variable spreading factor are disabled and replaced with AMC and fast packet scheduling. Also with the removal of fast power control, soft handovers cannot be performed with HSDPA data channels.

The principle of AMC is that depending on the channel quality the base station adapts the code rate and modulation type of the HS-DSCH channel as well as the number of channels allocated to one UE. This gives enough flexibility so that the variable SF and power control are not needed. Fast packet scheduling utilizes the 2 ms TTI to react very quickly to changing conditions and data rate needs. The channel quality is estimated by the UE and signalled to the BS in the form of a channel quality indicator (CQI).

3.3 Changes to network architecture

The basic structure of the network remains the same as in section 2.2; a HSDPA network contains all the same elements and interfaces as a Release '99 network. The biggest change is several RNC functionalities have been moved to the BTS: retransmissions, link adaptation and packet scheduling. The RNC must consequently be modified so that it allows the BTS to perform these tasks. In most cases both the BTS and the RNC can be updated to HSDPA with software updates. Some older models might need some hardware updates as well.

The Uu interface between the BTS and UE will change considerably to support new channels, coding and modulation types. The Iub interface between the BTS and the RNC will remain pretty much unchanged, the largest practical difference is that there will be considerably less retransmission traffic transmitted through the interface.

User equipment will have to be completely new with hardware and software changes. Older Release '99 terminals will be completely compatible with HSDPA networks, but they cannot naturally use any of the HSDPA features.

3.4 Changes to radio protocol architecture

HSDPA has very little effect on the protocol architecture described in section 2.3. Because all the major changes are made near the physical layer, the architecture changes also affect only Layer 1. In Release '99 retransmissions are done from the RNC. With HSDPA and HARQ the retransmission is handled by the BTS, as explained in section 3.3. This is illustrated in Figure 3-1. A new layer of logic in the

form of a new MAC layer is introduced to the base station: HSDPA Medium Access Control (MAC-hs). This new layer handles HARQ functionality, scheduling and priority handling for the HS-DSCH. The old MAC layer located in the RNC still maintains all of its old functions, including ARQ retransmissions in case HARQ fails. The MAC-hs layer is the only change required by HSDPA to the RAN architecture.
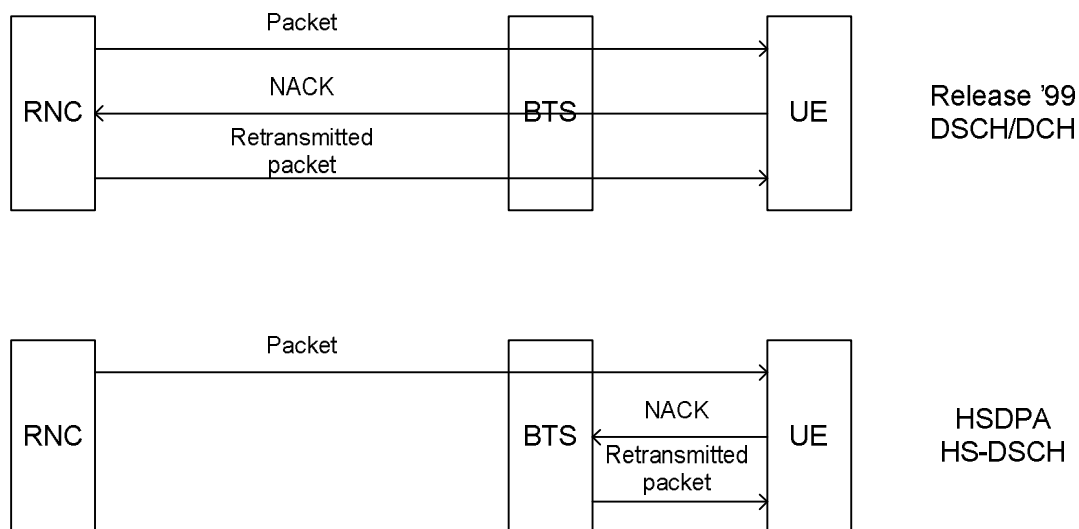
Figure 3-1: Retransmission schemes for Release '99 and HSDPA

3.5 Physical Layer

In Release '99 DCH and DSCH channels were paired together to offer flexible services. DCH carries data with tight delay requirements such as speech and DSCH carries rest of the user data. A similar pairing is used in HSDPA, where new HSDPA transport channels are paired with DCH. The DCH still uses Release '99 features such as fast power control and soft handover and is mainly used to transport speech. The HS-DSCH is used to transport larger data amounts like multimedia files. Because the HS-DSCH is superior to the DSCH, 3GPP removed the older channel from Release 5 and onwards.

The HS-DSCH is the only new transport channel introduced by HSDPA. In addition two downlink physical channels are added: The high-speed physical downlink shared channel (HS-PDSCH) carries the data on the HS-DSCH and the high-speed shared control channel (HS-SCCH) carries the HSDPA control data. Finally the uplink high-speed dedicated physical control channel (HS-DPCCH) carries HSDPA control information in the uplink.

3.5.1 High-Speed Downlink Shared Channel

HS-DSCH is used to carry user data and it has a peak data rate of 21.6 Mbps (14.4 Mbps before Release 7). It uses the short HSDPA TTI length of 2 ms (three slots). It has a fixed spreading factor. Some basic features of the channel can be seen in Table 3-1.

Table 3-1: Properties of HS-DSCH

Spreading factor	16, fixed
TTI	2 ms
Modulation types	QPSK, 16-QAM, 64-QAM
Coding scheme	Turbo coding

All of the new HSDPA features mentioned in Section 3.2 are used with HS-DSCH: HARQ, fast packet scheduling and AMC. Because of the fixed spreading factor, there are 16 channel codes available every TTI. However, only 15 HS-DSCH channels can be in use simultaneously because the 16th code is reserved for other channels such as DCH and CPICH. The HS-DSCH channels can be allocated to the users in range at will, and multiple codes can be allocated per user. The BTS has the responsibility to select the best transport format, modulation type and number of channels for each user. The type of the UE also affects the number of channels, because only high-end models support 15 parallel data channels.

Figure 3-2: QPSK, 16-QAM and 64-QAM constellations
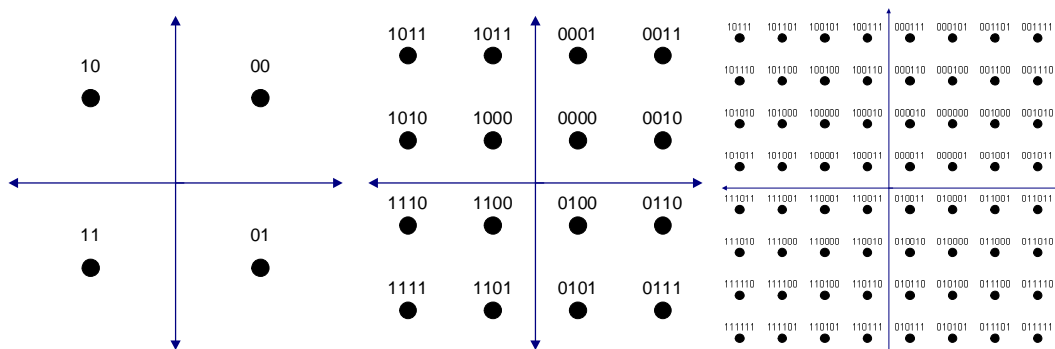
Originally HSDPA supported two different modulations: QPSK and 16-QAM. Release 7 added support for 64-QAM. The modulation constellations and bit mappings can be seen in figure 1. AMC can change the modulation type at each TTI. The higher order modulations carry more information but require better channel conditions. QPSK, 16-QAM and 64-QAM carry 2, 4 and 6 information bits per

symbol. Demodulation of 64-QAM is the main challenge of this thesis, and will be covered in chapter 4.

The fixed spreading factor, adapting modulation and short TTI allow the peak data rate of 21.6 Mbps. One slot consists of 2560 chips, so there are 7680 chips in a HSDPA TTI (= 3 slots). Because of the fixed spreading factor there are a total of 7680 / 16 = 480 symbols transmitted every TTI. With 64-QAM modulation 6 bits can be coded to each symbol. Remembering that TTI length is 2 ms and there can be at most 15 channels allocated to one user, the maximum throughput is:

480 symbols · 15 channels · (6 bits / symbol) / 2 ms = 21.6 Mbps **(2)**
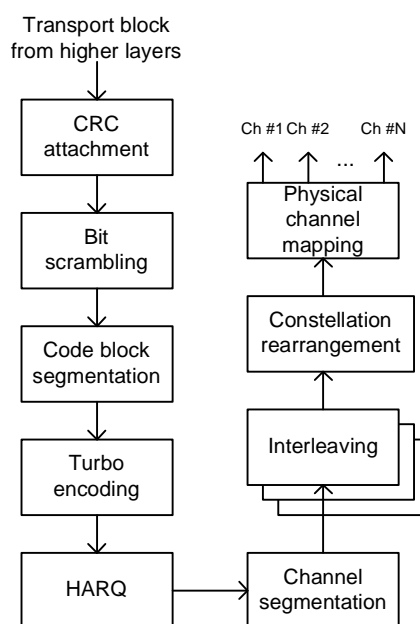
Figure 3-3: HS-DSCH coding chain

HS-DSCH is coded somewhat simpler than Release '99 physical channels (section 2.5.3), the coding chain can be seen in Figure 3-3. The Cyclic Redundancy Check (CRC) is the same as before. Because HS-DSCH in the only transport channel used with HSDPA, there is no need for transport channel multiplexing. Additionally because there are only 2 ms TTIs (as opposed to 10, 20, 40 and 80 ms in Release '99), there is only need for one interleaving block (the inter-column permutation). Rate matching is handled in HARQ.

With HS-DSCH convolutional coding is left out so that the only coding scheme is turbo coding. Because of AMC the code rate (number of encoded bits actually sent) can be changed every 2 ms, and by varying the transport block sizes code rates of 0.15-0.98 become available. The code rate is varied according to channel

conditions, because higher rates lower coding gain and require more error-free transmissions. In practice code rates between ¼ and ¾ are used.

Interleaving is dependent on the modulation. When QPSK is used, the interleaver is identical to the Release '99 interleaver. When 16-QAM is used, two identical interleavers are used in parallel, the second one interleaves the two extra bits brought by 16-QAM. Respectively, three interleavers are used for 64-QAM.

HARQ is a completely new feature on this level. On the receiver side, if a packet is received but the CRC check fails, the received data is stored in the HARQ buffer and a retransmission is requested. This request is sent in the uplink in the form of a one-bit ACK/NACK message (Acknowledgement / Not Acknowledged). If a retransmitted packet is received it is then combined with the old one. This is repeated until the correct packet is received or the maximum number of retransmissions is reached. If the reception fails even after HARQ, RNC-level retransmissions will occur. The retransmitted packet can be identical to the first one or ordered in a slightly different way. The different orderings have been standardized and are dependent on a redundancy version parameter set by the BTS.

The basic HARQ principle can be seen in **Figure 3-4**. The sent packets are stored in the buffer until the UE has received the packet correctly. Bit separation separates the actual user data (systematic bits) from the bits created by the turbo encoding (parity bits). The two-stage rate matching controls the bit flow in and out of the buffer. The first rate matching makes sure that the buffer does not overflow by limiting the inputs to the buffer. The second rate matching matches the number of outgoing bits to the number of physical channel bits available. The second rate matching also changes the order of the bits depending on the redundancy version.
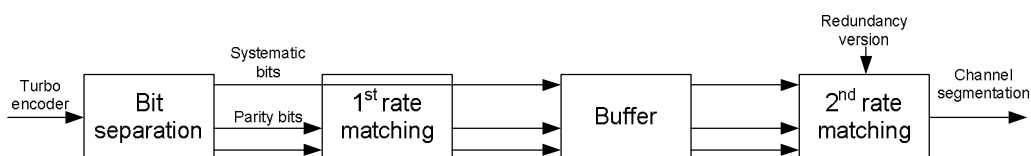
Figure 3-4: HARQ principle

New operations in the coding chain also include bit scrambling and constellation rearrangement. Physical layer bit scrambling is used to prevent too long sequences of 1s and 0s. Because power estimation algorithms generally assume that both bits are equally probable, long sequences of the same symbol should be avoided. Power estimation is covered in Chapter 4. Constellation rearrangement is used because different bits sequences have different demodulation probabilities with 16-QAM and

64-QAM. The bits are therefore rearranged before modulation so that HARQ retransmissions would help the detection of different bits evenly.

3.5.2 High-Speed Shared Control Channel

HS-SCCH carries the physical layer control information necessary to receive the data sent on HS-DSCH. HS-SCCH is sent if data is being transmitted on the HS-DSCH. There needs to be at least one HS-SCCH allocated per user, up to four may be used simultaneously. HS-SCCH has a fixed spreading factor of 128 and it uses QPSK modulation and half rate convolutional coding. The channel contains the following information about the data sent on the HS-DSCH:

- Modulation scheme

- Channelisation code and UE identity

- Transport block size

- HARQ process information

- Redundancy version and used constellation rearrangement scheme

This is all the information needed for the reception of HS-DSCH data. Parameters not sent, like the code rate, can be calculated from the sent parameters (for example the code rate can be calculated from the transport block size).

As with HS-DSCH, one HS-SCCH block is transmitted every HSDPA TTI (3 slots). The block is further divided into two parts: the first slot is called Part 1 and the two last slots Part 2. Part 1 contains the channelisation code and modulation type, the most time-critical pieces of information needed when HS-DSCH is first received. Part 2 contains the less time-critical information like transport block size and CRC of the HS-SCCH channel. Every UE in range will receive and decode Part 1 of every HS-SCCH packet sent by the BTS, but Part 2 will be ignored if the channel is not meant for that UE. Channels meant for different terminals are separated by UE specific masking in Part 1.

3.5.3 Uplink High-Speed Dedicated Physical Control Channel

In Release '99 the DPCH channel carried layer 1 control information in the uplink. Because HSDPA must work together with older releases, this old control channel was not modified and a new uplink control channel, HS-DPCCH, was added to carry HSDPA control information from the UE to the BTS. This channel sends ACK/NACK messages for HARQ retransmissions and Channel Quality Information (CQI). HS-DPCCH is multiplexed together with the DPCCH and DPDCH channels, and uses

some of the transmission power allocated to DPCCH. The channel has a fixed SF of 256 and uses half-rate convolutional coding.

CQI is a 5-bit figure that indicates the maximum transport format that the UE can reliably receive. The transport format is a combination of a channel's attributes, including modulation, transport block size and number of channels allocated to one user. Calculating the actual CQI value is quite complex and in addition to channel quality must take into account terminal capabilities [3GPP_214]. There is no standardized way to choose transmission type from the CQI and it is generally up to the network operator.

3.5.4 HSDPA timing

When HSDPA data is about to be sent, parameters for the HS-DSCH channel are received from the MAC-hs layer. These parameters are then mapped to the HS-SCCH channel. Because the time-critical information contained in part 1 of the HS-SCCH is needed before the HS-DSCH is received, the HS-SCCH is transmitted two slots before the HS-PDSCH carrying the HS-DSCH. The terminal has one slot to decode the necessary parameters.

After the HS-PDSCH is received, the appropriate HS-DPCCH channel is sent in the uplink 7.5 slots later. If it indicates a NACK, a retransmission will have to be sent on another HS-SCCH/HS-PDSCH pair. There is however no specification on how soon the retransmission will be sent, it is dependent on the capacity of the terminal. Some can receive data continuously while other terminals require up to 3 TTIs processing time before receiving the next packet. The timing relationship between all channels can be seen in Figure 3-5.
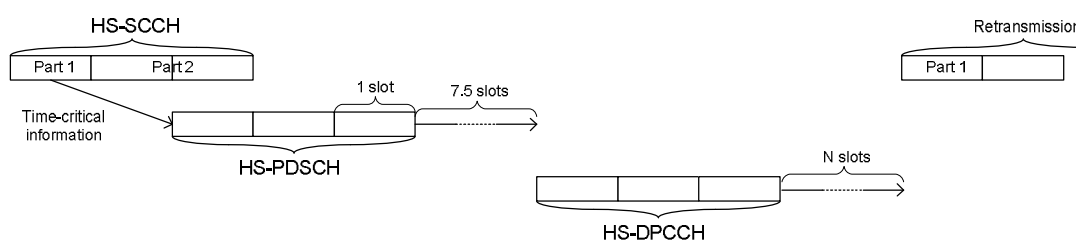

Figure 3-5: HSDPA channel timing

3.5.5 HSDPA data transmission procedure

This section describes how HSDPA data is sent from the BTS to a user. At every TTI the BTS knows the following information about all the users in a sector:

- Channel conditions (indicated by CQI)

- How much data is pending for the user (both retransmissions and new data)

- How long ago was the user last served

- Terminal limitations (modulation types, number of codes, HARQ memory etc.)

Depending on these and possibly other (vendor-dependent) factors the BTS decides how many channels to allocate for each user and which modulation and packet size to use. The exact way this is determined has not been standardized and is up to the network operator.

The BTS starts sending HS-SCCH two slots before HS-DSCH. If there was HS-DSCH data sent to the user in the previous TTI, the same HS-SCCH is used. Otherwise a new HS-SCCH may be selected from the available codes. All terminals decode Part 1 from all sent HS-SCCH channels. If the channel is recognized as meant for the user, Part 2 and the corresponding HS-DSCH frame are also received. The symbols in the frame are deinterleaved, demodulated, rearranged and put into the HARQ buffer. Depending on the parameters decoded from HS-SCCH the packet is either stored as new data or combined with an existing packet. The packet is turbo decoded and a CRC check is performed to make sure that the packet was received correctly. Depending on the CRC result an ACK or a NACK is sent back to the BTS on the HS-DPCCH channel. In parallel to all this, a CQI value is calculated from the CPICH signal.

4. ALGORITHMS

4.1 Introduction

The objective of this thesis is to find the best way to demodulate a 64-QAM modulated signal. In pre-Release 5 all data was modulated with QPSK modulation. Release 5 introduced HSDPA and the option of 16-QAM modulation. 16-QAM allowed twice the data to be transported on one symbol, but respectively introduced many new challenges. It is no longer enough to check the sign of the incoming symbol, but the magnitude of the symbols must also be estimated so that the correct bits can be decoded. In addition phase estimation requirements are much stricter because the constellation symbols are nearer to each other than in QPSK. Additionally because AMC can modify the channels every TTI, the magnitude must be estimated at least every 2 ms.

64-QAM doesn't present new challenges as such, but it makes the amplitude and phase estimation requirements even stricter. The constellation symbols are again much closer to each other, and an efficient estimation algorithm becomes more important. Constellation of all three modulation types can be seen in Figure 3-2.

This thesis focuses on two of the new challenges: threshold estimation and demodulation. To decode the constellation correctly, the magnitude of the symbols must be known. Since in HSDPA it is not signalled in any way, it has to be estimated from the data itself. Therefore threshold estimation is used to find the decision thresholds between the symbols in the constellation. The demodulation algorithm uses the threshold and the incoming symbol to decode six bits, and give estimates on how sure the decision is in the form of soft bits. The algorithm candidates presented in this chapter will be compared in Chapter 5. The problem of phase estimation is ignored in this thesis, and it is assumed that the constellations are not skewed.

The algorithm blocks are situated between despreading and HARQ. The incoming chips are despread into symbols as explained in Chapter 2. The symbols are first stored in a buffer so that the threshold can be estimated. The estimated threshold is then used to demodulate the symbols in the buffer, and the symbols are sent to HARQ. The relationship between the algorithms will be described in more detail in Chapter 5.

4.2 Threshold estimation

4.2.1 Introduction

Table 4-1: Summary of threshold estimation

Algorithm	Threshold estimation
Inputs	Despread data symbols
Outputs	Threshold estimate
Parameters	Estimation time, estimation channels, modulation type, number of channels

A summary of the threshold estimation algorithm can be seen in Table 4-1. Data symbols can arrive on several different channels (up to 15). The algorithm must know the number of used data channels to receive the correct amount of data.
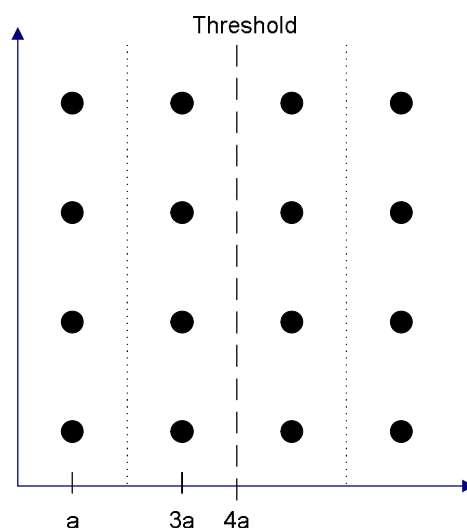
Figure 4-1: 64-QAM decision threshold

The output is the threshold estimate. The upper right part of the 64-QAM constellation can be seen in Figure 4-1. The decision threshold in the I-branch has been drawn with a dashed line. The axis amplitude of the first signal is marked as *a*. It can be seen that in an ideal case, the threshold can be calculated as in equation (3). Calculating one threshold is enough, because the other two decision thresholds can be calculated either by multiplying or dividing the threshold. The other two thresholds can be seen in the figure as dotted lines. Because of symmetry the same thresholds can be used in all quadrants. Additionally, because I and Q should have

the same power there is no need to calculate separate thresholds for I and Q. This has been confirmed in 4.2.2.4.

$$Thr = 4 \cdot a \tag{3}$$

Two of the parameters, estimation time and estimation channels, basically determine how much estimation data is available. When symbols are received, they are buffered until a threshold estimate has been calculated. In HSDPA modulation can be changed every TTI (2 ms), so the estimation time cannot be longer. In practice the threshold can change even faster due to fading channels and mobility. That is why estimation time should generally be shorter than one TTI. Again if estimation time is too short the estimate becomes too inaccurate due to a lack of estimation data. An estimation period of one slot (160 symbols) will be used in the simulations.

One way to gain better accuracy without using more time is to use symbols from all used data channels. Because transmission power is same for all channels within one frame and the channels are received simultaneously, there is a gain of more estimation data with no downsides. It must be remembered however that there are not always multiple data channels in use, so relying only on multiple channels for estimation accuracy is a mistake.

4.2.2 Algorithm candidates

4.2.2.1 Power estimation

This algorithm candidate estimates the power of the incoming signal with very basic mathematic formulas. That power estimate is then transformed into the threshold with a method derived in this section.

The signal power will be calculated as *decision point power* defined in [3GPP_141] DPP is the sampled power of a limited set of complex symbols. It is defined as

$$P = mean(| x |^2) \tag{4}$$

where x is the set of data symbols for estimation. If there are N symbols received in the estimation period, and power is estimated from K channels, the DPP can be calculated with equation (5). $x(n,k)$ is the nth received symbol in the estimation period from channel k. Because x is a two-dimensional complex symbol consisting of I and Q, the amplitude can be calculated with equation (6). $x_I(n,k)$ is the I-component of the incoming signal and $x_Q(n,k)$ the Q-component.

$$\overline{P} = \frac{\sum\limits_{n=0}^{N-1}\sum\limits_{k=0}^{K-1}\left|x(n,k)\right|^2}{NK} \tag{5}$$

$$\left|x(n,k)\right| = \sqrt{x_I(n,k)^2 + x_Q(n,k)^2} \tag{6}$$

Using equation (5) DPP can also be calculated for the ideal 64-QAM constellation with one occurrence of each symbol. The upper right quadrant can be seen in Figure 4-2. The positions of the symbols are marked along the axes.
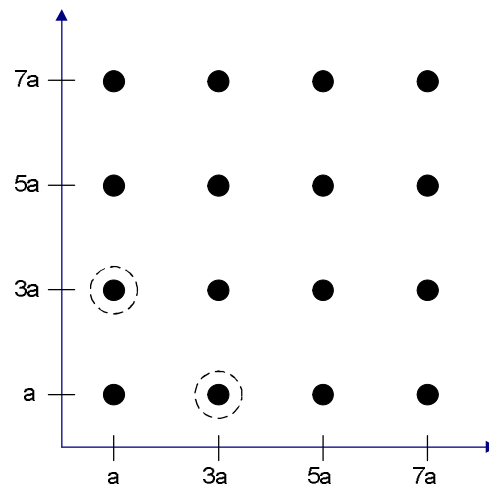
Figure 4-2: 64-QAM symbol amplitudes

There are a total of 64 symbols in the constellation. The power of the bottom left symbol is $(a^2 + a^2)$, and because of symmetry there are 4 symbols with that power in the whole constellation. The power of the two circled symbols is $(a^2 + 9a^2)$, and there are 8 such symbols in the whole constellation. Continuing through the whole quadrant, the power of the entire constellation can be calculated as in equation (7). P is the power of an ideal 64-QAM constellation with one occurrence of each symbol.

$$P = \frac{4 \cdot (a^2 + a^2) + 8 \cdot (a^2 + 9a^2) + 4 \cdot (9a^2 + 9a^2) + 8 \cdot (a^2 + 25a^2) + 8 \cdot (a^2 + 49a^2) + 8 \cdot (9a^2 + 25a^2)}{64}$$
$$+ \frac{8 \cdot (9a^2 + 49a^2) + 4 \cdot (25a^2 + 25a^2) + 8 \cdot (25a^2 + 49a^2) + 4 \cdot (49a^2 + 49a^2)}{64} = 42a^2 \tag{7}$$

Turning this equation around, we get an equation for the axis amplitude of the first symbol that is dependent only on the power of the constellation

$$a = \sqrt{\frac{P}{42}} \tag{8}$$

Combining equations (3) and (8), an expression for the threshold can be formed:

$$Thr = 4 \cdot a = 4 \cdot \sqrt{\frac{P}{42}} \tag{9}$$

This threshold is only dependent on the power of the constellation. Finally, replacing *P* with the estimate from equation (5), a formula for calculating the threshold from the incoming symbols can be formed:

$$Thr = \frac{4}{\sqrt{42}} \sqrt{\frac{\sum_{n=0}^{N-1} \sum_{k=0}^{K-1} \left| x_{in}(n,k) \right|^2}{NK}} \tag{10}$$

This equation is based on the assumption that there is an equal probability for receiving each symbol. Although in reality this almost never holds exactly, if the group of estimation symbols is large the symbol distribution is uniform enough.

4.2.2.2 Amplitude estimation

This algorithm candidate works very much like power estimation. The only difference is that instead of estimating power, the amplitude of the incoming symbols is estimated. So now the variable to be estimated is

$$A = mean(| x |) \tag{11}$$

As before, the mean is estimated from all channels in the estimation period:

$$\overline{A} = \frac{\sum_{n=0}^{N-1} \sum_{k=0}^{K-1} \left| x(n,k) \right|}{NK} \tag{12}$$

The only difference between equations (12) and (5) is that the symbol amplitude is not squared. Equation (6) is still used to calculate the amplitudes.

As in power estimation, the amplitude estimate is now calculated for the ideal constellation. Again the only difference to the ideal power is that the amplitudes are inside square roots. The equation for the ideal amplitude can be seen in equation (13). Because of the square roots the relation between the amplitude and the axis position cannot be reduced, in practice a constant approximation must be used. That constant can also be seen in equation (13) with an accuracy of 8 significant digits. That should be enough accuracy for any practical system.

$$P = \frac{4 \cdot \sqrt{a^2 + a^2} + 8 \cdot \sqrt{a^2 + 9a^2} + 4 \cdot \sqrt{9a^2 + 9a^2} + 8 \cdot \sqrt{a^2 + 25a^2} + 8 \cdot \sqrt{a^2 + 49a^2} + 8 \cdot \sqrt{9a^2 + 25a^2}}{64}$$
$$+ \frac{8 \cdot \sqrt{9a^2 + 49a^2} + 4 \cdot \sqrt{25a^2 + 25a^2} + 8 \cdot \sqrt{25a^2 + 49a^2} + 4 \cdot \sqrt{49a^2 + 49a^2}}{64} \approx 6.08689047a \tag{13}$$

Finally, using the same principle as in power estimation, equations (3), (12) and (13) are combined to form an estimate for the threshold. That estimate can be seen in equation (14).

$$Thr = \frac{4}{6.08689047} \frac{\sum_{n=0}^{N-1} \sum_{k=0}^{K-1} |x(n,k)|}{NK} \tag{14}$$

4.2.2.3 Improved amplitude estimation

This algorithm candidate [Ced03] estimates the threshold directly from the one-dimensional axis amplitudes. Looking at the threshold in Figure 4-1, it is easy to see that the threshold is an average of the symbol positions on the axis:

$$Thr = 4 \cdot a = \frac{a + 3a + 5a + 7a}{4} \tag{15}$$

So this algorithm simply calculates the average of the axis positions. Because of symmetry, symbols from all quadrants and both I and Q can be used. Of course the absolute values of negative symbol positions will be used. The average can be simply calculated as:

$$Thr = \frac{\sum_{n=0}^{N-1} \sum_{k=0}^{K-1} \left(|x_I(n,k)| + |x_Q(n,k)| \right)}{2 \cdot NK} \tag{16}$$

The 2 in the divider is needed because two values are added from each symbol (I and Q). One major advantage of this algorithm is simplicity: there are no square roots or power calculations.

4.2.2.4 Other considered algorithm candidates

There were some other algorithm candidates considered, but they were eliminated early due to bad results in preliminary simulations. These results will not be presented, but the algorithms will be shortly described here with reasons for discarding them.

One idea was to calculate individual thresholds for I and Q. Although I and Q should have the same power, there might be differences due to the randomness of the data. The improved amplitude estimation (section 4.2.2.3) was used to calculate the individual thresholds. It turned out that the results were always worse when compared to combined threshold estimation. The reason for this is most likely that

the amount of estimation data halved because two thresholds had to be estimated from the same group of data. It is also likely that the thresholds for I and Q are on average close enough that no separate thresholds are needed.

In another tested method the thresholds were calculated for each quadrant separately and then averaged. This had no notable effect on the results but increased complexity. Therefore there was no need to do further simulations related to that idea.

4.3 Demodulation

4.3.1 Introduction

Table 4-2: Summary of 64-QAM demodulation

Algorithm	64-QAM Demodulation
Inputs	Despread data symbols, threshold estimate
Outputs	Soft bits
Parameters	None

The demodulation algorithm produces 6 bits from each incoming symbol. The symbols are stored in a buffer while the thresholds are estimated, and are then sent to the demodulator.

The mapping of the bits to the constellation can be seen in Figure 4-3 [3GPP_213]. If the threshold is known, decoding the correct *hard bits* (= zeros and ones) is a trivial task. One must only compare the position of the incoming symbol to the thresholds. But in this case the outputs of the demodulator are *soft bits* or *soft decisions*. Soft bits are numbers in which the sign tells the hard bit value (0 or 1) and the absolute value indicates the reliability of the decision. Each algorithm candidate in the following sections produces a measure for how probable the hard bit is.

These soft bits have two functions. First of all in case of retransmissions they are combined in HARQ. This way the most reliable bits are selected from each frame. Secondly the turbo decoder can decode the signal better when it has the bit probabilities to work with.
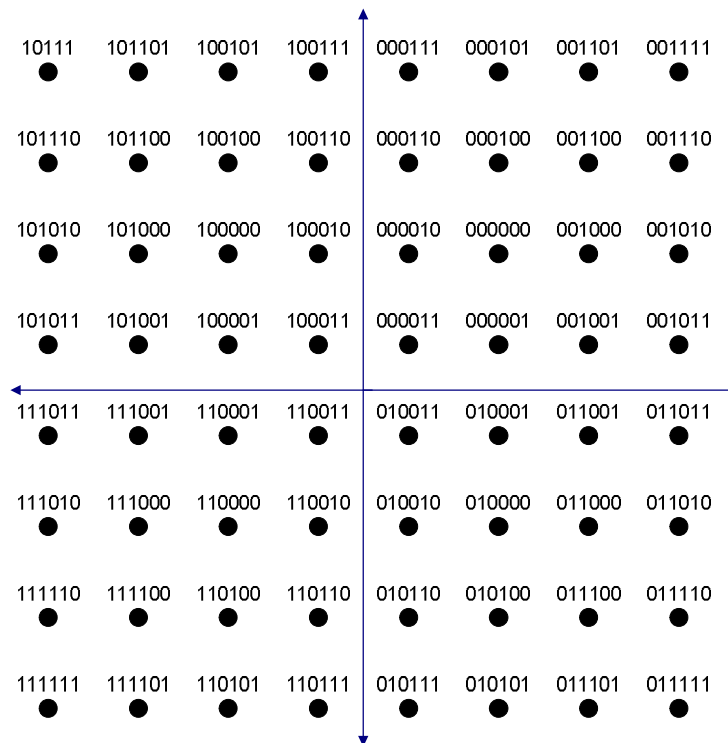
10111	101101	100101	100111	000111	000101	001101	001111
●	●	●	●	●	●	●	●
101110	101100	100100	100110	000110	000100	001100	001110
●	●	●	●	●	●	●	●
101010	101000	100000	100010	000010	000000	001000	001010
●	●	●	●	●	●	●	●
101011	101001	100001	100011	000011	000001	001001	001011
●	●	●	●	●	●	●	●
111011	111001	110001	110011	010011	010001	011001	011011
●	●	●	●	●	●	●	●
111010	111000	110000	110010	010010	010000	011000	011010
●	●	●	●	●	●	●	●
111110	111100	110100	110110	010110	010100	011100	011110
●	●	●	●	●	●	●	●
111111	111101	110101	110111	010111	010101	011101	011111
●	●	●	●	●	●	●	●

Figure 4-3: 64-QAM mapping

The 64-QAM constellation can be divided into several different partitions based on what bit each symbol represents. Let the six demodulated bits be $\{b_1 b_2 b_3 b_4 b_5 b_6\}$, the mapping for which can be seen in Figure 4-3. For each bit b_i, there are 32 symbols in the constellation that indicate a zero and another 32 that indicate a one. Let S_i be the group of points indicating that $b_i = 0$ and $\overline{S}_i$ the group indicating that $b_i = 1$. For example, S_1, S_3 and S_5 can be seen in Figure 4-4. The constellation group symbols can be calculated with the threshold estimate from the previous algorithm, remembering the definition of *a* from equation (3). So for example the upper right symbol of the constellation is

$$s = 7/4 \cdot Thr + 7/4 \cdot Thr \cdot i \qquad (17)$$

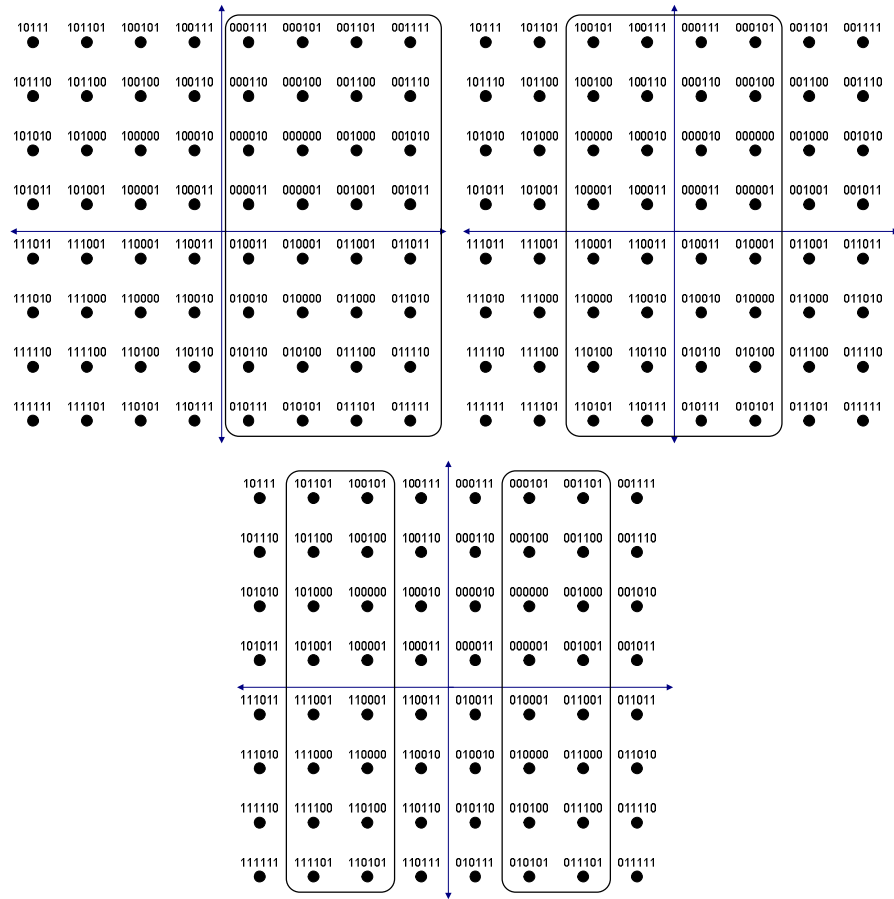and so on. These groups will be used in the following algorithms.

Figure 4-4: Constellation point groups S_1 (top left), S_3 (top right) and S_5

4.3.2 Algorithm candidates

4.3.2.1 Full log likelihood demapper

This algorithm candidate demodulates the signal with a maximum a posteriori (MAP) optimum detector described in [Zie00]. Let b_i be the bit to be demodulated and x the incoming symbol. The incoming symbol is one of the constellation points polluted with AWGN noise. b_i can now be selected with the rule

$$b_i = 0 \text{ if } P(b_i = 1 \mid x) < P(b_i = 0 \mid x), \ b_i = 1 \text{ otherwise} \tag{18}$$

where $P(b_i = 0 \mid x)$ is the probability that b_i is 0 given x. Equation (18) can be written as

$$b_i = 0 \text{ if } \frac{P(b_i = 0 \mid x)}{P(b_i = 1 \mid x)} > 1, \ b_i = 1 \text{ otherwise} \tag{19}$$

The division in the equation is called the *likelihood ratio*. The probability that b_i is 0 can be indicated with the groups defined in 4.3.1, and the likelihood ratio becomes

$$\frac{P(b_i = 0)}{P(b_i = 1)} = \frac{P(s \in S_i)}{P(s \in \overline{S}_i)} \tag{20}$$

where *s* is a variable that can be any symbol in the constellation. Now a function for the likelihood ratio must be derived. According to [Pro01], using the Bayes theorem the ratio may be expressed as

$$\frac{P(s \in S_i)}{P(s \in \overline{S}_i)} = \frac{\sum_{s \in S_i} p(x \mid s)}{\sum_{s \in \overline{S}_i} p(x \mid s)} \tag{21}$$

where *p(x)* is the probability density function (pdf) of *x*. This density function must be derived so that the likelihood ratio can be calculated.

The constellation is polluted with AWGN noise. The pdf of a Gaussian distribution is

$$p_G(x) = \frac{1}{\sigma\sqrt{2\pi}} \exp\left\{-\frac{(x-\mu)^2}{2\sigma^2}\right\} \tag{22}$$

where σ is the noise variance and μ the mean. Now let us consider the incoming symbol *x*. In Figure 4-5 an incoming symbol is marked with a cross and its distance to the nearest constellation point *s* is marked with *d*. Now the probability density function of *x* given *s* is a function of the distance, as seen in equation (23). d(s,x) is the squared Euclidean distance between *x* and *s*.
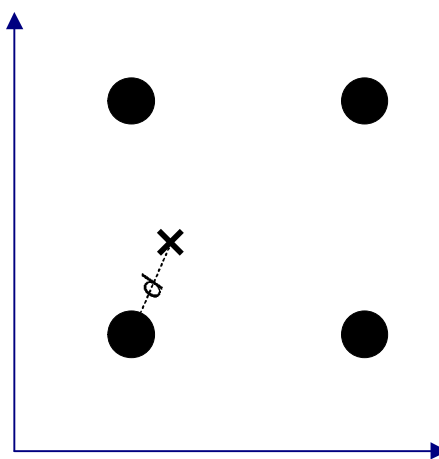

Figure 4-5: Distance of incoming symbol to two constellation points

$$p_G(x \mid s) = \frac{1}{\sigma\sqrt{2\pi}} \exp\left\{-\frac{d(x,s)}{2\sigma^2}\right\} \tag{23}$$

The equation is the probability density function of the incoming symbol, assuming that the symbol it represents is *s*. This can be combined with equation (21) to calculate the likelihood ratio of an incoming bit. The decision rule now becomes:

$$b_i = 0 \text{ if } \frac{\sum_{s \in S_i} \frac{1}{\sigma\sqrt{2\pi}} \exp\left\{-\frac{d(s,x)}{2\sigma^2}\right\}}{\sum_{s \in S_i} \frac{1}{\sigma\sqrt{2\pi}} \exp\left\{-\frac{d(s,x)}{2\sigma^2}\right\}} > 1, \; b_i = 1 \text{ otherwise} \tag{24}$$

This can be somewhat simplified. The common multiplier $1/\sigma\sqrt{2\pi}$ can be removed. In addition it is beneficial to take a logarithm of the whole likelihood, forming a *logarithmic likelihood ratio* (LLR). The final decision rule therefore becomes

$$b_i = 0 \text{ if } \log \frac{\sum_{s \in S_i} \exp\left\{-\frac{d(s,x)}{2\sigma^2}\right\}}{\sum_{s \in S_i} \exp\left\{-\frac{d(s,x)}{2\sigma^2}\right\}} > 0, \; b_i = 1 \text{ otherwise} \tag{25}$$

This is dependent on the incoming symbol, the estimated constellation and the noise variance. When these are known, all bits can be demodulated.

But as explained in 4.3.1, the outputs of the algorithm are soft bits. The LLR in equation (25) can be used as a soft bit value. It is positive when hard bit 0 is more likely, and its magnitude gets larger when the decision is more certain.

4.3.2.2 Max-log MAP demapper

The full log likelihood is optimal in a Bayesian sense if the constellation is polluted with AWGN noise. However, it has several downsides. It is extremely heavy to calculate and is also highly dependent on correct estimation of the noise variance. Noise is estimated from the signal by the UE, so it is never ideal. The Max-log algorithm candidate is based on the assumption that the largest value dominates in the logarithmic sum [Tos01]. Therefore the LLR in equation (25) can be simplified to:

$$LLR_{ML}(b_i) = \log \frac{\max_{s \in S_i} \exp\left\{-\frac{d(s,x)}{2\sigma^2}\right\}}{\max_{s \in S_i} \exp\left\{-\frac{d(s,x)}{2\sigma^2}\right\}} \tag{26}$$

Because the exponent and the maximum-operation are commutative (maximum of an exponent = exponent of a maximum), they can switch places. We now get:

$$LLR_{ML}(b_i) = \log \frac{\exp \max_{s \in S_i}\left\{-\frac{d(s,x)}{2\sigma^2}\right\}}{\exp \max_{s \in S_i}\left\{-\frac{d(s,x)}{2\sigma^2}\right\}} \tag{27}$$

The division inside the logarithm can be turned into a subtraction:

$$LLR_{ML}(b_i) = \log \exp \max_{s \in S_i} \left\{ \frac{-d(s, x)}{2\sigma^2} \right\} - \log \exp \max_{s \in \bar{S_i}} \left\{ \frac{-d(s, x)}{2\sigma^2} \right\} \tag{28}$$

The logarithm and exponent cancel each other out. In addition the negative signs can be removed by turning the maximum-operations into minimum-operations. We now get:

$$LLR_{ML}(b_i) = \min_{s \in S_i} \left\{ \frac{d(s, x)}{2\sigma^2} \right\} - \min_{s \in \bar{S_i}} \left\{ \frac{d(s, x)}{2\sigma^2} \right\} \tag{29}$$

The constant $1/2\sigma^2$ can be taken to the front as a common factor. The simplified way to calculate the ith soft bit of symbol x is now:

$$LLR_{ML}(b_i) = \frac{1}{2\sigma^2} \left\{ \min_{s \in S_i} d(s, x) - \min_{s \in \bar{S_i}} d(s, x) \right\} \tag{30}$$

This still fills the requirements for a soft decision. It is positive when 0 is more probable, and its absolute value gets bigger when the decision is more confident. It is also much lighter to calculate than the full log likelihood.

4.3.2.3 Simplified Demapper

This algorithm candidate reduces the max-log algorithm to a one-dimensional problem [Tos01]. It is extremely light but it also simplifies the problem somewhat.

Looking at the constellation mapping in Figure 4-3 and the example groups in Figure 4-4, it can be seen quite easily that all the individual bit decision thresholds are either horizontal or vertical and span the entire constellation. This information can be used to formulate a simpler demodulation algorithm. Remember that the I-axis is the real axis and the Q-axis the imaginary axis.

Let the six demodulated soft bits be $\{s_1 s_2 s_3 s_4 s_5 s_6\}$. The first two bits are defined by the signs of I and Q. The next two bits are 0 if the absolute value of the axis position is smaller than the threshold. The last two bits are 0 on the two symbol rows closest to the threshold. These rules are visualized for the I-axis in Figure 4-4. The formula for calculating the soft bits can be seen in equation (31).

$$s_1 = \mathrm{Re}\{x\}$$
$$s_2 = \mathrm{Im}\{x\}$$
$$s_3 = Thr - \mathrm{Re}\{x\}$$
$$s_4 = Thr - \mathrm{Im}\{x\}$$
$$s_5 = Thr/2 - \big\|\,\mathrm{Re}\{x\}\,|\,-Thr\big|$$
$$s_6 = Thr/2 - \big\|\,\mathrm{Im}\{x\}\,|\,-Thr\big|$$

(31)

The one-dimensional distances also fill all the soft decision requirements. They are positive when the decision is 0, and they grow when the decision is more confident.

4.3.2.4 Other demodulation algorithms

It was initially decided that no other demodulation algorithms would be considered than the ones mentioned here. A study made for local area networks with 64-QAM [Tos01] has shown that in practice the simplified demapper works just as well as the theoretically ideal algorithm. Because of the very low complexity of the algorithm compared to its reported performance, it didn't seem worthwhile to search for other algorithms. If the results for HSDPA would be considerably different, it would be worthwhile to look for better algorithms. However, as the results in Chapter 5 will show the simplified demapper indeed gives almost ideal performance. Therefore at this time there is no need to look for a better algorithm.

4.4 Complexity

This section will give a short analysis of the complexities of the different algorithms, adding one more factor to consider when selecting the best algorithm.

4.4.1 Threshold Estimation

The complexity of estimating the threshold from N symbols and K channels will be considered here. For power estimation the first operation is calculating the squared amplitude of each symbol. Because the symbols are complex, there are a total of N·K sums and N·K squares. The amplitudes are then summed together, causing another N·K sums. The result is then divided with both N and K and a square root is taken. Finally, the result is multiplied with a constant.

Amplitude estimation is otherwise the same as power estimation, except that the square root is taken before the sum. Therefore instead of one square root operation, there are N·K square roots.

Improved amplitude estimation then again is very simple. The absolute value of both I and Q is taken from every symbol, resulting in 2·N·K absolute operations. These

are all summed together, requiring 2·N·K sums. The result is divided by both N and K and multiplied with a constant.

The amount of operations for each algorithm can be seen in Table 4-3. Amplitude estimation is somewhat more complex than power estimation because of the large amount of square roots. Improved amplitude estimation and power estimation have about the same amount of operations. The only difference is that in power estimation there are 2·N·K squares and in the other algorithm 2·N·K absolute operations. This means that improved amplitude estimation is somewhat lighter than power estimation, since taking the absolute value is simpler than squaring.

Table 4-3: Complexities of the threshold estimation algorithms

Algorithm	Sums	Multiplications	Divisions	Squares	Square roots	Absolute
Power Estimation	2·N·K	1	2	2·N·K	1	0
Amplitude estimation	2·N·K	1	2	2·N·K	N·K	0
Improved AE	2·N·K	1	2	0	0	2·N·K

4.4.2 Demodulation

The complexity of demodulating 6 soft bits from one symbol will be considered here. The operation *distance* will be used, meaning the two-dimensional Cartesian distance requiring two subtractions, two squares and one square root operation.

The full log likelihood requires 64 distances to be calculated, the distances of the incoming symbol to each constellation point. Each of those distances will then be multiplied with a constant, causing 64 multiplications. Then the exponent will be taken from each result, causing 64 operations. The likelihoods of the two groups will then be summed and divided, causing 64 sums and one division. Finally, a logarithm is taken from the result.

With max-log MAP the 64 distances will also have to be calculated. Otherwise the algorithm is simpler, requiring only two minimum-operations, one subtraction and one multiplication with a constant. The simplified demapper on the other hand requires only six subtractions, two multiplications with a constant and four absolutes.

A summary of the complexities can be seen in Table 4-4. There is a clear order in the complexities, with the full log likelihood being the most complex and the simplified demapper the most simple.

Table 4-4: Complexities of the demodulation algorithms

Algorithm	Sums	Multi	Divisions	Exp	Distance	Minimum	Abs	Logarithm
Full log likelihood	64	64	1	64	64	0	0	1
Max-log MAP	1	1	0	0	64	2	0	0
Simplified demapper	6	2	0	0	0	0	4	0

5. SIMULATION STUDY

5.1 Problem statement

The goal of this thesis is to find the best way to demodulate a 64-QAM modulated signal in HSDPA. The algorithms will be compared in different scenarios using throughput as a measure. Throughput means the data rate of the transmitted user data. There is always a fixed number of bits transmitted every TTI per channel, but some of those bits are always error coding bits.

5.2 Simulation environment

5.2.1 Simulator

The simulations will be run on a Layer 1 HSDPA simulator. Random bits are generated, and they are mapped to HS-DSCH channels and modulated as explained in section 3.5.1. The channels are then spread and scrambled and other necessary channels (SCH, HS-SCCH, CPICH, PICH, PCCPCH and DPCH) are multiplexed to the signal. If less than 15 HS-DSCH channels are used, other data channels are modelled with an Orthogonal Channel Noise Simulator (OCNS) [3GPP_101]. The signal is corrupted with either AWGN noise and phase error or a fading channel, modelled with a FIR filter.

The receiver model can be seen in Figure 5-1. The received signal is first filtered in a LMMSE equalizer to counter the channel [Nok04]. The equalizer signal is then correlated with the spreading code of the UE in the Despreader to distinguish the HS-DSCH channel(s) meant for the UE (see section 2.4.1). The corresponding HS-SCCH channel is also separated from the signal.
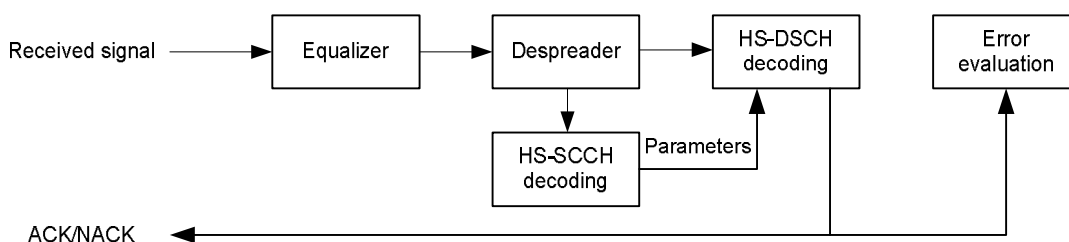

Figure 5-1: Receiver model

Parameters like modulation type and number of channels are decoded from the HS-SCCH, and the actual transmitted data bits are decoded according to Figure 5-2. Then the symbols are first buffered so that the threshold estimator can calculate the decision thresholds. Those thresholds are then used in the demodulator to demodulate the symbols in the buffer. Rest of the chain consists of inter-column

deinterleaving, HARQ, turbo decoder and the CRC check. If the CRC fails, the whole transport block is discarded and a retransmission is requested and combined in HARQ.
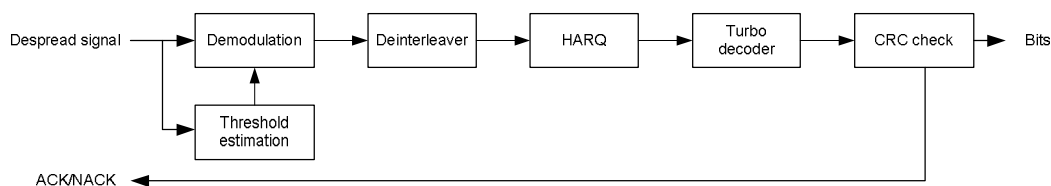

Figure 5-2: HS-DSCH decoder model

Algorithm candidates for threshold estimation and demodulation are compared. Performance of the algorithms is compared with throughput as defined in [3GPP_101]: "Number of information bits per second excluding CRC bits successfully received on HS-DSCH by a HSDPA capable UE." The throughput can be calculated from the block error rate (BLER) as explained in the following example. BLER means the relative number of discarded TTIs.

Since one transport block is transmitted every TTI, the maximum throughput can be calculated by dividing the used transport block size with 2 ms. If the CRC check fails, a NACK is sent and the whole block is discarded. So for example if the used transport block size is 26600 bits and the BLER 0.15, the throughput is:

$$Tput = 26600b / 0.002s \cdot (1 - 0.15) = 11.3 Mbps$$

The throughput will be plotted as a function of geometry (I_{or} / I_{oc}). Geometry is the power ratio between transmit power and the power of noise sources. Noise can be for example thermal noise, inter-symbol interference and interference from other sectors. Geometry effectively expresses how noisy the signal is. As the geometry rises, the throughput begins to saturate because all bits are decoded correctly. There are no differences between the algorithms in the saturated areas. For each case the geometry values will be selected so that the throughput has not reached the maximum.

5.2.2 Parameters

5.2.2.1 Base station transmit power

To simplify defining standard transmit power, 3GPP has defined that for simulations the total base station transmit power (I_{or}) equals 1. Therefore powers of all downlink physical channels transmitted from the base station must sum to unity. In

other words equation (32) must hold, where P_i is the transmit power for channel *I* in decibels.

$$\sum_{i=Channels} 10^{P_i/10} = 1 \qquad (32)$$

The powers of all channels used in the simulations can be seen in Table 5-1. The powers for P-CPICH, P-CCPCH, SCH and PICH are taken from downlink physical channel definitions by 3GPP (section C.5.1 of [3GPP_101]). Note that usually in HSDPA P-CCPCH and SCH share the same transmit power. However since SCH caused unnecessary noise in the results, that channel was turned off. The powers for HS-PDSCH, HS-DSSCH and DPCH are taken from 3GPP 64-QAM minimum requirements (section 7.4.2.2 of [3GPP_101]). OCNS is selected so that equation (32) holds.

Table 5-1: Physical channel powers

Physical channel	Channel power (dB)
P-CPICH	-10
P-CCPCH	-12
SCH	-100
PICH	-15
HS-PDSCH	-2
HS-SCCH	-13
DPCH	-13
OCNS	-11.3

These channel powers will be used for all simulations, with one exception. When there are 15 HS-DSCH channels in use, there can be no other traffic channels in use. Therefore OCNS power is set to -100, which effectively means it is off. Because the transmit powers must still sum to 1, DPCH is modified to fulfil equation (32). So when 15 data channels are used, channel powers from Table 5-2 will be used.

Table 5-2: Physical channel powers with 15 HS-DSCH channels

Physical channel	Channel power (dB)
DPCH	-9.6
OCNS	-100

5.2.2.2 Radio Channel type

Two different channel models will be used for the simulations. First, an AWGN channel with no multipath propagation whatsoever. This channel type is used to maximize the effect of the algorithms on the throughput. When a multipath channel is used, errors caused by fading might overshadow differences between the algorithms. In practice an AWGN channel is very rare, it occurs mainly in test laboratories, open areas near base stations and picocell areas such as internet cafes. A picocell is a base station designed for very small areas, such as one room. Although an AWGN channel is quite rare, it is not trivial. It is on these channels that the highest throughputs promised by HSDPA are reached.

However it is good to test the algorithms in more realistic situations. Because 64-QAM is used mainly in very good channel conditions, a simple Rayleigh fading channel model called Pedestrian A 3 km/h [ITU_1225] is used. This channel is also used for the HSDPA 64-QAM minimum requirements set by 3GPP [3GPP_101].

5.2.2.3 Data channel type

Although in real situations the transport block size, modulation and number of channels can change every TTI, these parameters will be fixed for each simulation run. This is done to eliminate all other variables except for the algorithm itself.

For the AWGN channels, a very high code rate is used. This is because on high block sizes even small errors cause large changes in throughput. A high code rate is therefore good for comparing algorithms. Different numbers of channels are used to compare performance with different amounts of estimation data for the threshold estimation algorithms.

For the more realistic Pedestrian A 3 channel, a more reasonable code rate will be used. The code rate used in the 3GPP 64-QAM requirement specifications is 0.61, so it will also be used here. Information about the different scenarios can be seen in Table 5-3, the block sizes have been taken from the list of allowed HS-DSCH transport block sizes [3GPP_321].

Table 5-3: Transport block sizes

Number of channels	Channel type	Code rate	Transport block size
15	AWGN	0.98	42192
10	AWGN	0.97	27960
5	AWGN	0.97	13920
1	AWGN	0.97	2784
15	Pedestrian A 3	0.61	26600
10	Pedestrian A 3	0.61	17568
1	Pedestrian A 3	0.61	1744

5.2.2.4 Other parameters

This section lists all other used simulation parameters. Since these simulations model a high-end Category 14 terminal, data is sent every TTI and a maximum of 4 HARQ retransmissions are used. HSDPA terminal categories are explained in e.g. [Hol07] section 12.6. Redundancy version 6 is used in the constellation re-arrangement and HARQ combining, since it is also used in the 3GPP requirements. For all simulations, a total of 10000 sub-frames will be sent to minimize random errors.

Table 5-4: Other simulation parameters

Parameter	Value
Inter-TTI interval	1
Maximum number of HARQ retransmissions	4
Redundancy version	6
Number of transmitted sub-frames	10 000

One important variable is noise added to the data symbols to be demodulated, because it is a variable in two of the demodulation algorithms (full log likelihood and max-log MAP). The noise can be calculated with the geometry (I_{or} / I_{oc}). Since I_{or} was defined in equation (32) to be 1, noise at the receiver can be defined as:

$$I_{oc} = 1/G \qquad (33)$$

Where G is the geometry. Before this noise affects the symbols themselves the signal goes through the despreader. Because the spreading factor is 16, the signal power is amplified 16-fold or approximately 12 dB (as explained in chapter 2). Now according to Table 5-1 the power of the HS-DSCH channel where the symbols are transmitted is -2 dB. That power is furthermore divided among all used transport channels. The noise is on the other hand evenly divided between these channels. Therefore the value used as the variance of noise in the demodulation can be calculated as:

$$\sigma^2 = \frac{10^{-2/10}}{NumCh \cdot 10^{-(G+12)/10}} \tag{34}$$

Where *NumCh* is the number of used transport channels.

5.3 Simulation results

5.3.1 Threshold estimation

In these simulations the simplified demapper was used for demodulation. Results on the AWGN channel are presented first. Results for 15, 10, 5 and 1 data channels can be seen from Figure 5-3 to Figure 5-6. The abbreviations used in the figures in this chapter are listed in Table 5-5.

Table 5-5: Abbreviations used in the simulation figures

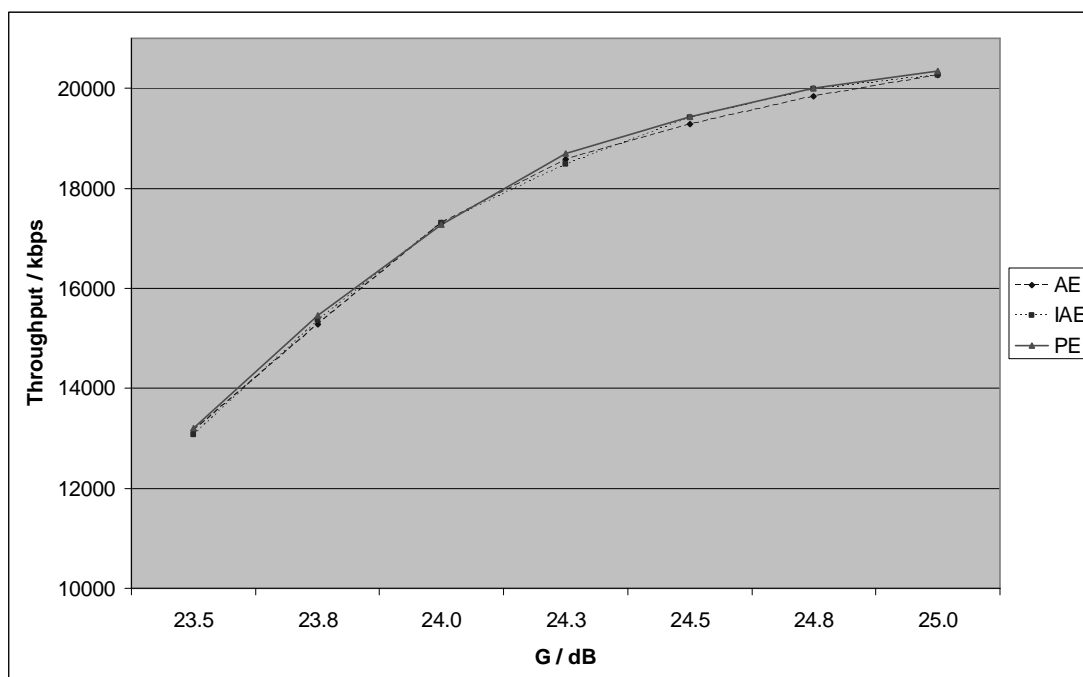| Abbreviation	Algorithm
AE	Amplitude estimation (4.2.2.2)
IAE	Improved amplitude estimation (4.2.2.3)
PE	Power estimation (4.2.2.1)
Full Log	Full log likelihood (4.3.2.1)
Max Log	Max-log MAP (4.3.2.2)
Simpl	Simplified demapper (4.3.2.3)

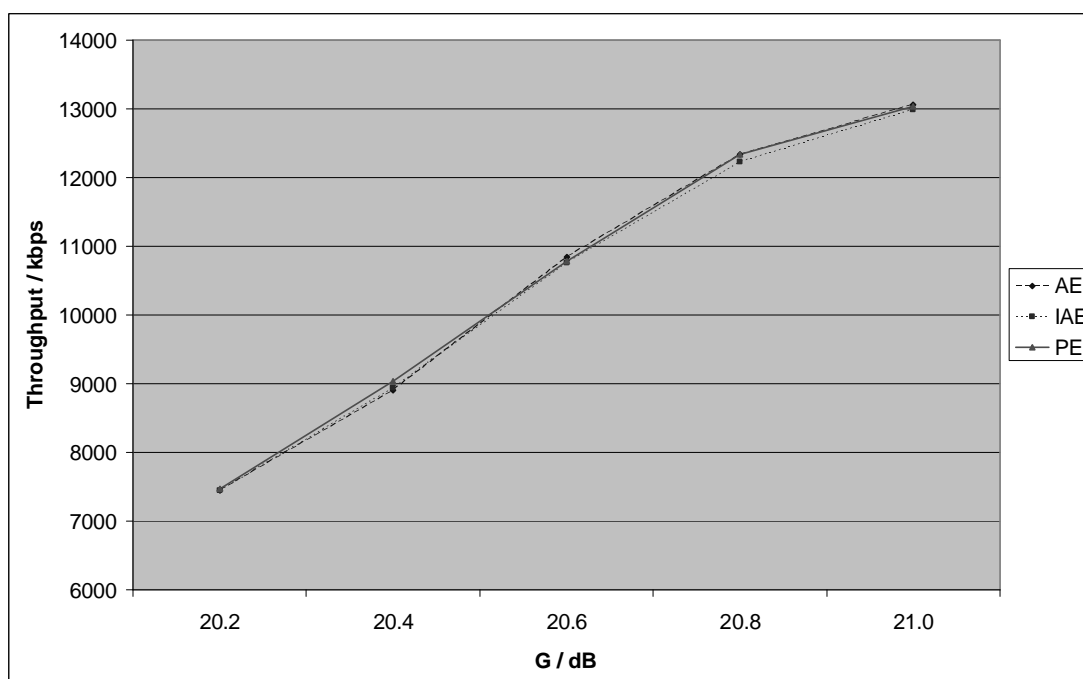**Figure 5-3: AWGN threshold estimation results with 15 channels**

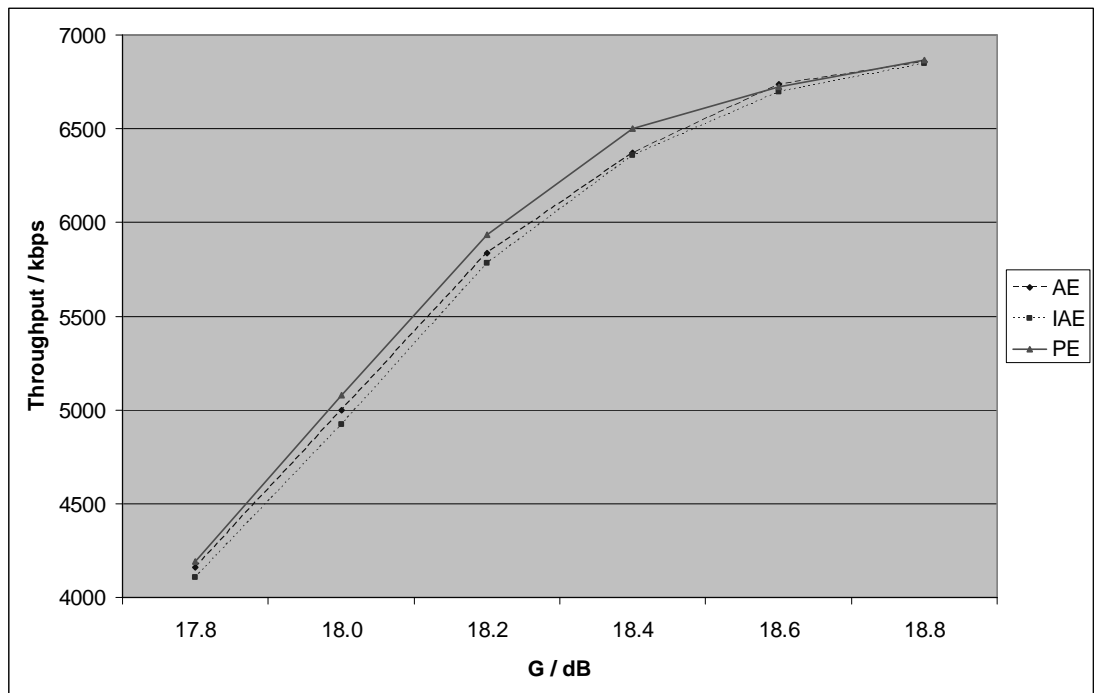**Figure 5-4: AWGN threshold estimation results with 10 channels**

Figure 5-5: AWGN threshold estimation results with 5 channels
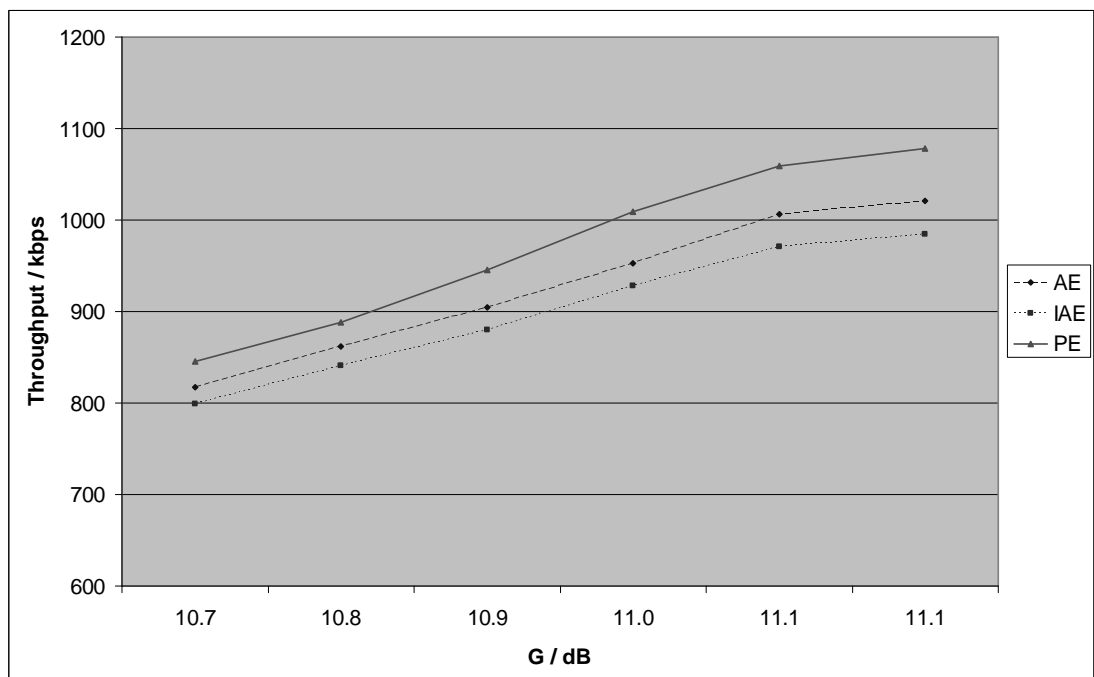

Figure 5-6: AWGN threshold estimation results with 1 channel

With 15 and 10 channels all algorithms give equal performance. With 5 channels power estimation is somewhat better than the other algorithms and amplitude estimation is a little better than improved amplitude estimation. With only one channel there is a clear order with power estimation being the best algorithm, amplitude estimation being the runner up and improved amplitude estimation giving the worst throughputs.

Sampo Pitkänen   52

The Pedestrian A 3 km/h simulations were run next. It turned out that these simulations offered nothing interesting. All algorithms gave practically the same performance, for example the 15 channel case can be seen in Figure 5-7. Since all the other figures looked exactly the same, they are not presented here. Analyzing the numerical results instead of the figures gives the same conclusion: the small throughput differences caused by the different algorithms are completely random. It seems that when a fading channel is used, there are so many other factors that cause errors that the demodulation is not a bottleneck.
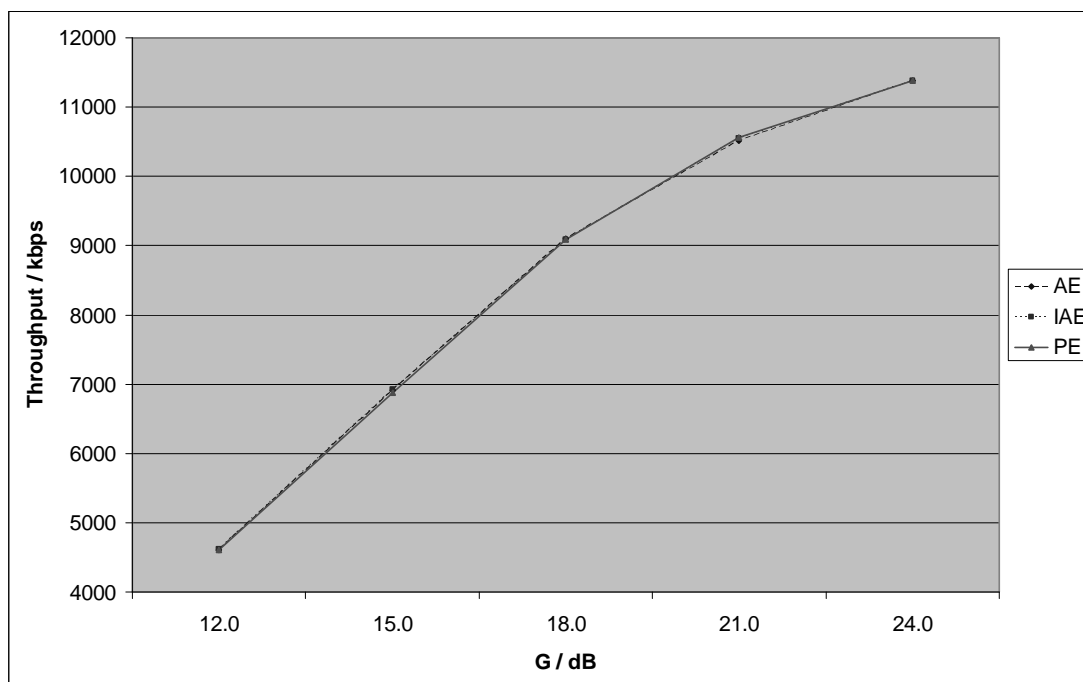

Figure 5-7: Pedestrian A 3 threshold estimation results with 15 channels

Because results on the fading channel give no information on the algorithms, the conclusions will be drawn from the AWGN results. It seems that when there is much estimation data available and high geometry, all algorithms are equally good. This makes sense, since with a very large set of estimation data all algorithms should give approximately correct results. Increasing the number of estimation symbols makes the symbol distribution more even, and all the algorithms were based on the assumption that all symbols are as good. Averaging over a large set of symbols also decreases noise. Since the threshold is estimated from one slot (160 symbols per channel), 15 and 10 channels give a set of 2400 and 1600 symbols to estimate from.

When there is less estimation data available, differences between the algorithms become apparent. Already with five channels (800 symbols) power estimation is

clearly better than the others. With only one channel (160 symbols) this difference continues to grow.

The number of channels is not the only variable in the simulations however. The power allocated to the HS-DSCH channels is split evenly between all used channels, so when fewer channels are in use each channel has more power. Therefore the geometry is lower in the simulations with a smaller amount channels. To isolate the variables of geometry and size of estimation data, two new simulations were run.

In the first simulation we look at a situation with high geometry but little estimation data. This was done by repeating the current AWGN case for 15 channels, but using only the samples from the first channel for threshold estimation. In real life this scenario might occur with slower terminals that due to limited processing power can not process all available estimation data in the given time frame. Results for this case can be seen in Figure 5-8.
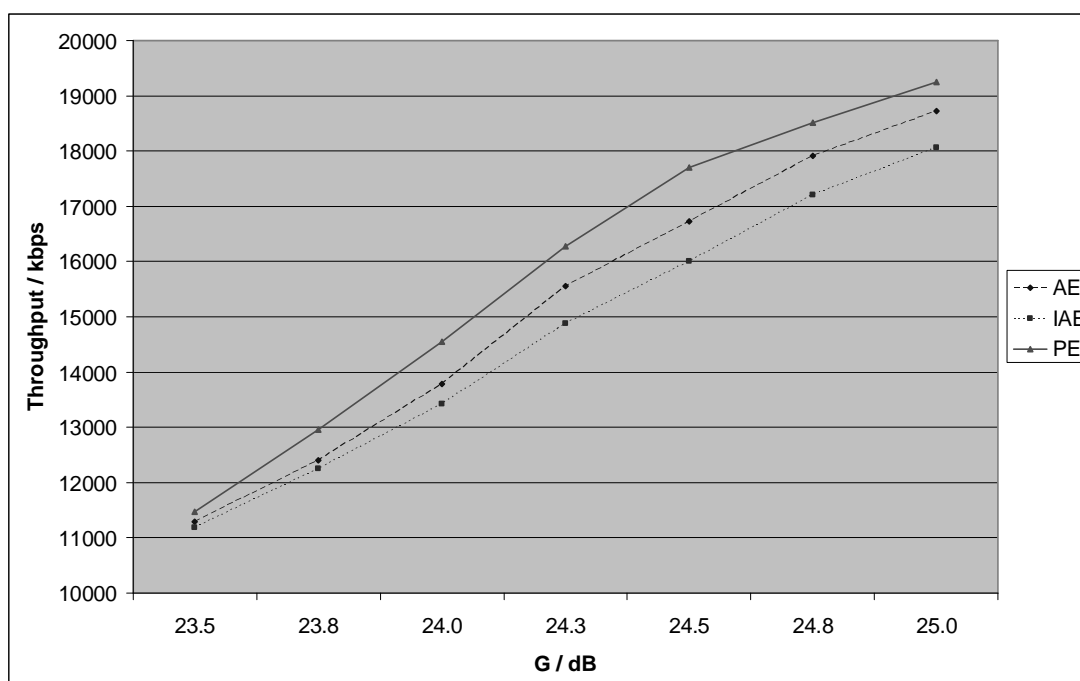

Figure 5-8: AWGN threshold estimation results with high geometry 1 estimation channel

The other case was that of low geometry and much estimation data. The geometry values from the AWGN one channel case were used, but the number of channels was set to 15. An appropriate code rate was selected so that the throughput wouldn't be saturated. The code rate used was 0.41 (transport block size 17568). The results for this simulation can be seen in Figure 5-9.

The first simulation confirms the dependency on the size of the estimation data set. Power estimation is clearly the best algorithm when only a few channels are in use. The second simulation however revealed a new dependency. It seems that power estimation performance begins to degenerate with low geometry. In the original simulations the amount of estimation data still gave the benefit to power estimation, but in this case it seems that the improved amplitude estimation algorithm is better.
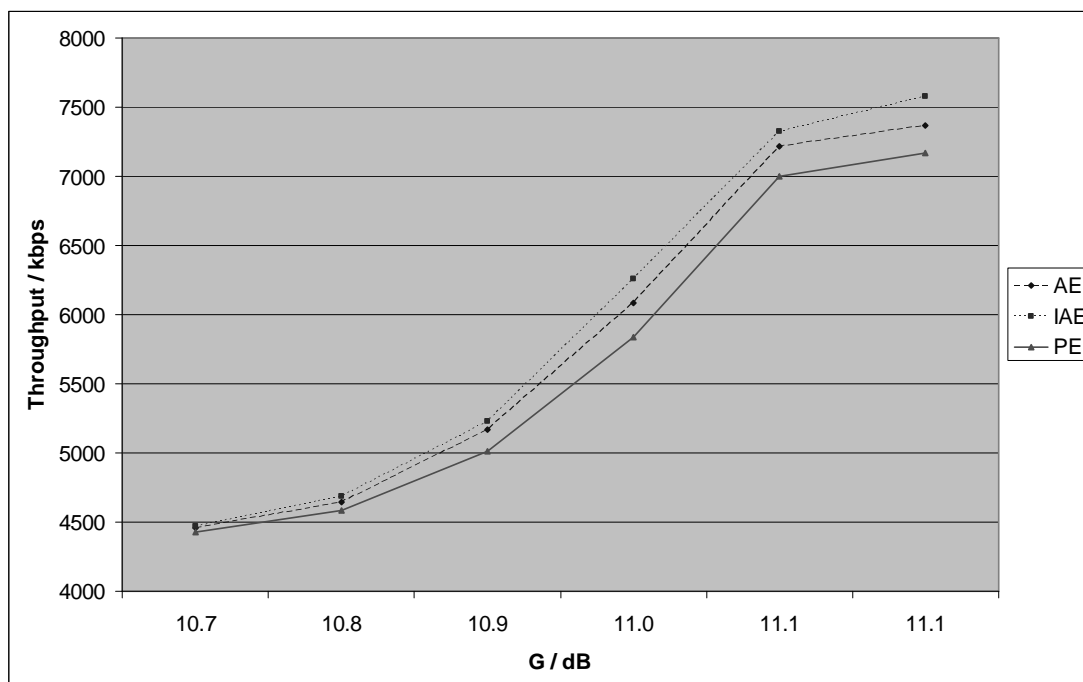

Figure 5-9: AWGN threshold estimation results with low geometry and 15 estimation channels

It seems that there is no clear answer as to which algorithm is the best. The only algorithm that can be clearly discarded is the amplitude estimation, since it never gives the best results and since according to section 4.4.1 it is also the most complex. The algorithm candidate to be selected would therefore be either power estimation or improved amplitude estimation.

The question now is which is more important: performance with a low number of channels or with low geometry. The choice could be done if there was some data available on how many channels on average are in use. However since during the writing of this thesis the first HSDPA networks supporting 64-QAM are years away, this data does not exist. Network operators and other telecommunications companies most likely already have strategies on how to distribute channels between users, but that information is not available to the public.

Therefore the only conclusion that can be made is that power estimation is best when there are only a few channels available while improved amplitude estimation is

better when the signal-to-noise ratio is low. An intuitive solution would be to implement both algorithms and select the better one based on the number of channels and channel quality since both variables are known at the receiver. This might however be more trouble than it is worth, since in the common fading channels all algorithms showed equal performance. In the end the choice is not a simple one, and depends on the goals and uses of the final product.

5.3.2 Demodulation

Power estimation was used for calculating the thresholds in this section. Simulations on the Pedestrian A 3 km/h channel gave similar results as in section 5.3.1: no differences between the algorithms whatsoever. The figures are not presented here since they offer no new information. There were also only very small differences on the AWGN channel, the results can be seen from Figure 5-10 to Figure 5-13.
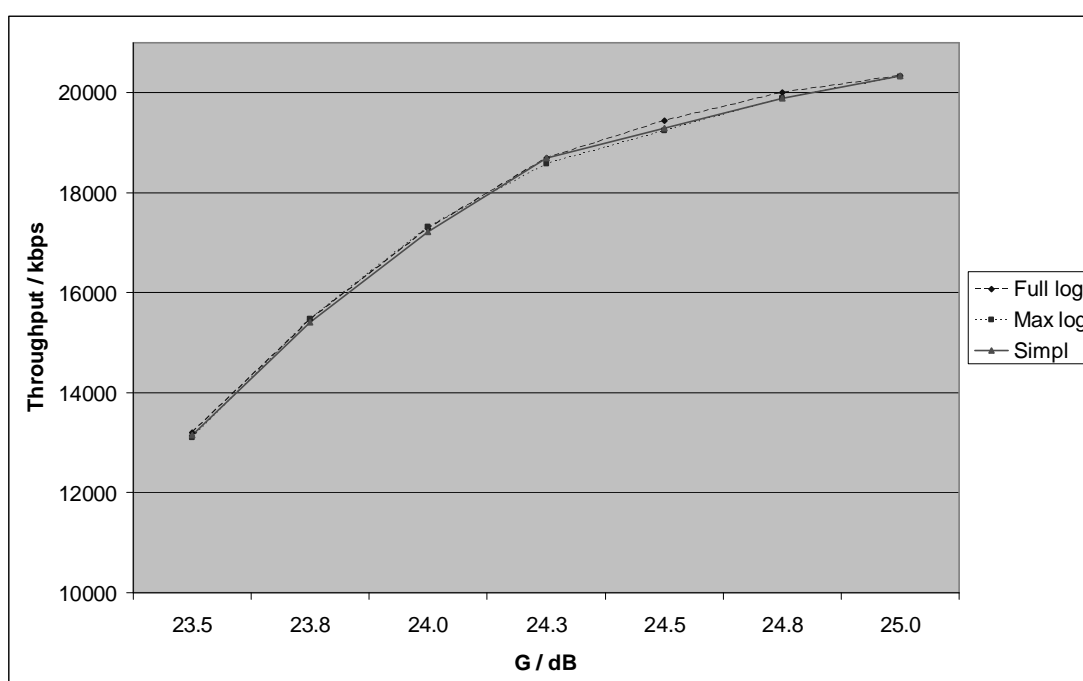

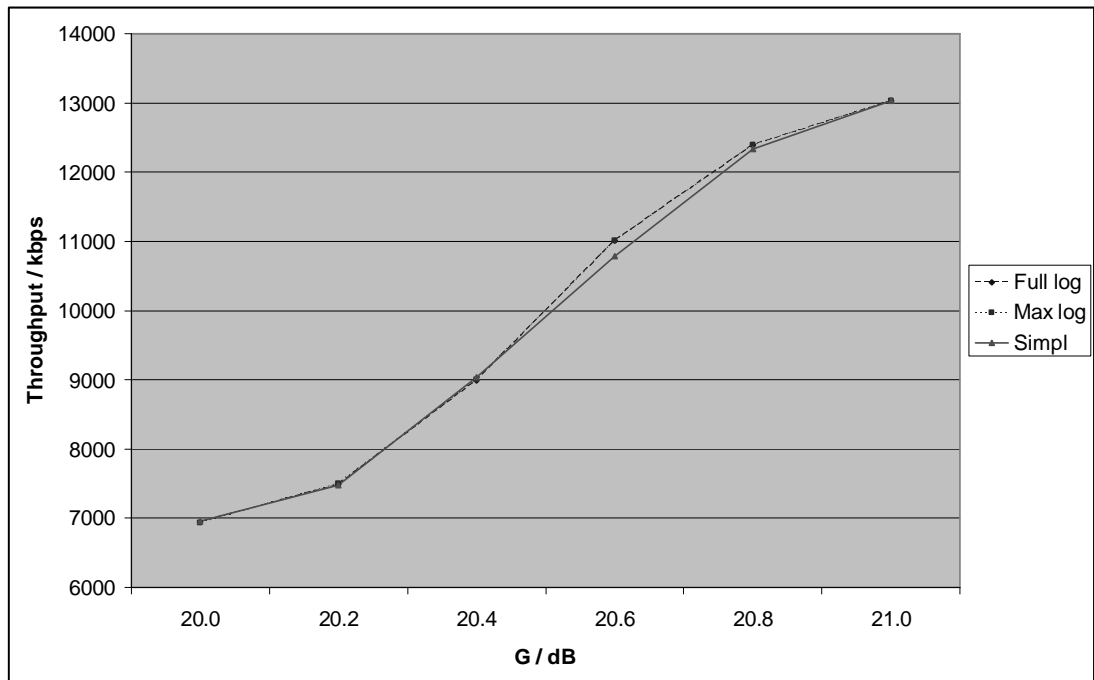**Figure 5-10: AWGN demodulation results with 15 channels**

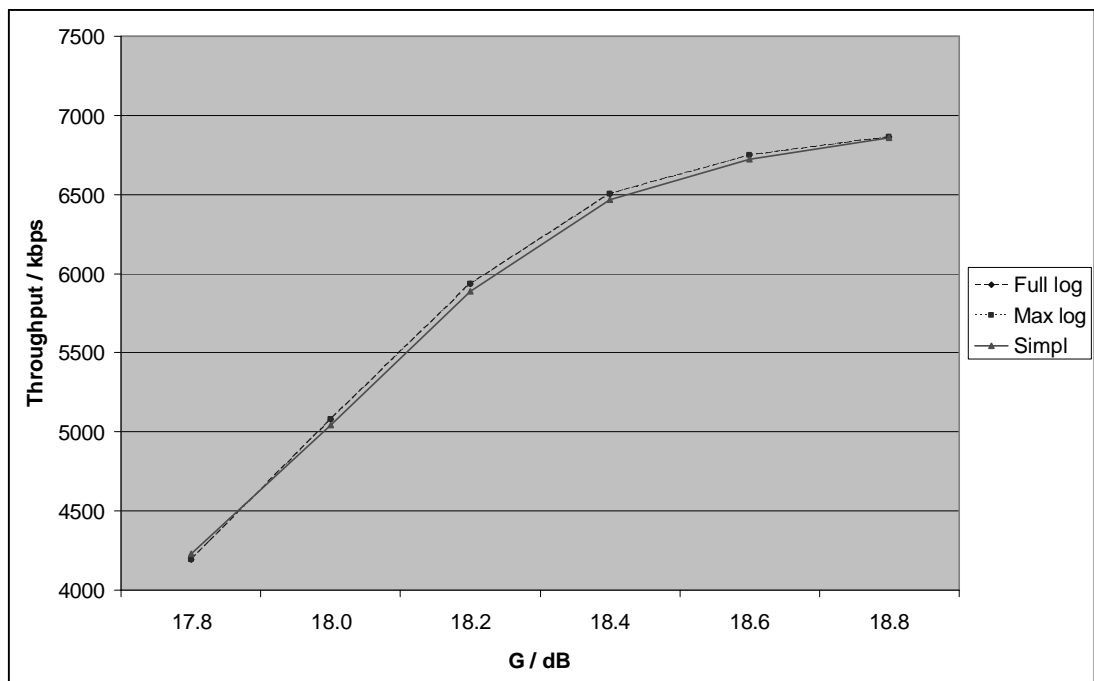**Figure 5-11: AWGN demodulation results with 10 channels**

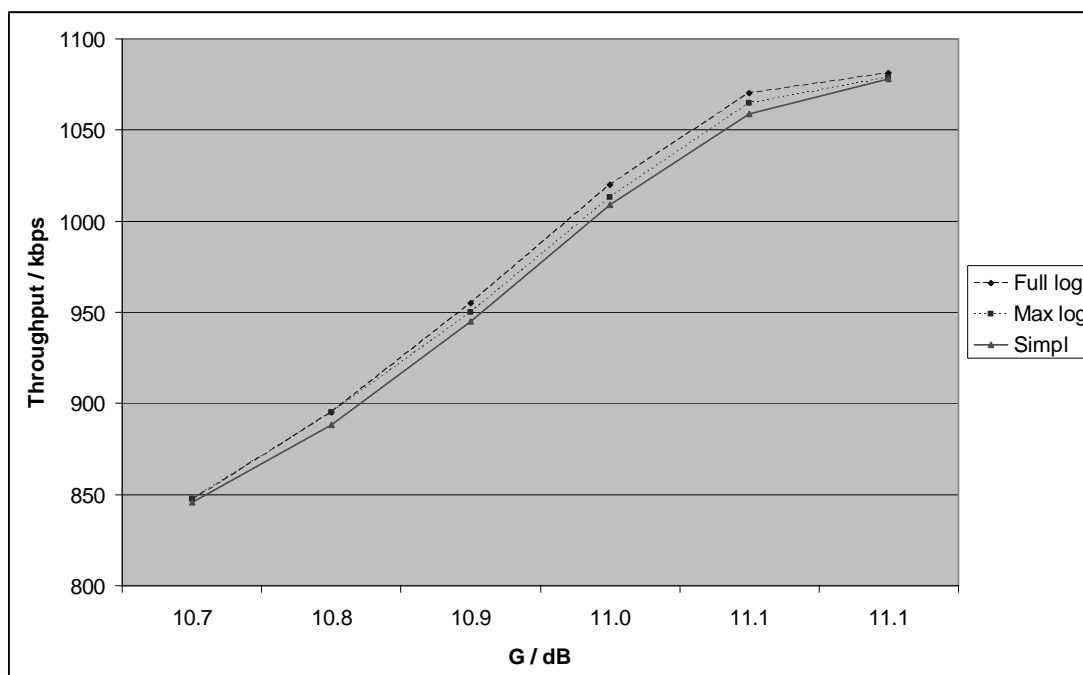**Figure 5-12: AWGN demodulation results with 5 channels**

Figure 5-13: AWGN demodulation results with 1 channel

There is a clear pattern throughout the figures: the ideal demapper gives the best performance while the max-log is practically as good. The simplified demapper decreases the throughput very slightly, but the difference is very minor. Remembering from section 4.4.2 that the simplified demapper is significantly less complex than the other algorithms, it seems that for all practical purposes it is the best candidate for demodulation. This is in line with other papers that have studied these algorithms, like [Tos01].

6. SUMMARY

This thesis studied the best way to receive a 64-QAM modulated signal in a HSDPA system. Chapter 2 gave an introduction to UMTS and WCDMA, focusing on the physical layer. Chapter 3 explained HSDPA in more detail. In chapter 4 the problem of demodulating 64-QAM was presented and different algorithms suggested. In chapter 5 the algorithms were compared with different simulations. Although some of the results were not as decisive as they could be, the best alternatives for receiving 64-QAM were found, thus fulfilling the goal of this thesis.

Demodulation of a 64-QAM signal can be divided into two subtasks: estimating the decision threshold and the actual demodulation with that threshold. Three algorithms were compared for the task of threshold estimation: power estimation, amplitude estimation and improved amplitude estimation. Three different algorithms were compared for the demodulation: full log likelihood, max-log MAP demapper and simplified demapper.

6.1 Conclusions

One common result for all simulations was that with fading channels, in this case Pedestrian A 3 km/h, using different algorithms made no difference whatsoever. This indicates that in common situations the algorithms used to demodulate 64-QAM are not a bottleneck. However in a rarer but still possible AWGN channel there were some clear differences between the algorithms.

With the threshold estimation algorithm candidates the amount of estimation data and channel quality proved to be the deciding factors. As with estimation in more general, a large amount of data increases estimation accuracy. So when in this case over 10 data channels were in use in good channel conditions, each algorithm had enough data to produce an accurate enough estimate. However in real life all data channels are not always active. When only few channels were used, in this case 1 and 5, the less complex algorithms showed a significant drop in performance. The less data there was available, bigger the gap between the algorithms became. Clearly the best results were given by power estimation.

However, power estimation seemed to have a lower tolerance to noise than the other algorithms. When channel quality was poor but all channels were in use, the improved amplitude estimation algorithm actually gave better performance. Therefore the selection of the best algorithm depends on the situation. When there are only a few channels in use, power estimation provided the best results. However

with a low signal-to-noise ratio and many channels, improved amplitude estimation proved to be the best. There is no decisive way to select the best algorithm for every case, so a model that implements both algorithms might be the best choice.

With the demodulation algorithm candidates the simulations were based on prior information. A study done for local area networks [Tos01] indicated that an extremely light demodulation algorithm for quadrature amplitude modulation gave practically as good results as the optimal MAP-detector. The goal was to confirm that this also applies to HSDPA, and possibly seek other algorithms if this is not the case. The results showed that the simplified demapper that reduces the demodulation to a one-dimensional problem indeed is practically as good as the optimal algorithm, so there is no need to look for better algorithms with HSDPA.

6.2 Further study

The results for demodulation were pretty clear, and therefore it seems that for the specific task of demodulating a 64-QAM signal in HSDPA there needs to be no further research.

The results for threshold estimation were not as clear since there were two good algorithm candidates with different strengths. Further research on a model that selects between the two algorithms might be beneficial. This model could monitor the number of data channels, channel quality and possibly other factors and select the algorithm. This would be outside the scope of this thesis however.

7. REFERENCES

[3GPP_101]   3GPP Technical Specification 25.101: User Equipment (UE) radio transmission and reception (FDD). www.3gpp.org. 25.09.2007

[3GPP_141]   3GPP Technical Specification 25.141: Technical Specification Group Radio Access Network; Base Station (BS) conformance testing (FDD). www.3gpp.org. 25.09.2007

[3GPP_211]   3GPP Technical Specification 25.211: Physical channels and mapping of transport channels onto physical channels (FDD). www.3gpp.org. 07.09.2007

[3GPP_212]   3GPP Technical Specification 25.212: Multiplexing and channel coding (FDD). www.3gpp.org. 26.09.2007

[3GPP_213]   3GPP Technical Specification 25.213: Spreading and modulation (FDD). www.3gpp.org. 26.09.2007

[3GPP_214]   3GPP Technical Specification 25.214: Physical layer procedures (FDD). www.3gpp.org. 26.09.2007

[3GPP_301]   3GPP Technical Specification 25.301: Radio interface protocol architecture. www.3gpp.org. 24.10.2007

[3GPP_321]   3GPP Technical Specification 25.321: Medium Access Control (MAC) protocol specification. www.3gpp.org. 24.10.2007

[Ada97]   Adachi, F., Sawahashi, M. and Okawa, K., 'Tree-structured generation of orthogonal spreading codes with different lengths for forward link of DS-CDMA mobile radio', *Electronics Letters*, 1997, Vol. 33, No. 1, pp. 27-28

[Ced03]   Cedergren A., Lindoff B. and Malm P. 'Method and system for M-QAM detection in communication systems', US patent No. 10609917, 2003

[Eri06a]   Ericsson. '64QAM for HSDPA – Link-Level Simulation Results'. TSG-RAN WG1 Meeting #46. R1-062264. www.3gpp.org. 23.08.2006

[Eri06b]   Ericsson. '64QAM for HSDPA – System-Level Simulation Results'. TSG-RAN WG1 Meeting #46. R1-062265. www.3gpp.org. 23.08.2006

[Hol06]   Holma, H. and Toskala A., 'HSDPA/HSUPA for UMTS', 2006, John Wiley & Sons, Ltd

[Hol07]   Holma, H. and Toskala A., 'WCDMA for UMTS – HSPA evolution and LTE', 4th edition, 2007, John Wiley & Sons, Ltd

[ITU_1225]   ITU-R. 'Recommendation M.1225. Guidelines for evaluations of radio transmission technologies for IMT-2000'. 1997. www.itu.int

[Nok04]   Nokia. 'HSDPA improvements for UE categories 7 and 8'. TSG RAN WG4 meeting # 33. R4-040680. www.3gpp.org. 15.11.2004

[Pro01]   Proakis J., 'Digital Communications'. 4th edition. 2001. McGraw-Hill Higher Education.

[Tos01]   Tosato F. and Bisaglia P., 'Simplified soft-output demapper for binary interleaved COFDM HIPERLAN/2', Proc. Of ICC 2002, IEEE Intl' Conf. on Commun. 2002, vol. 2, pp. 664-668.

[Zie00]   Ziemer R. and Peterson R., 'Introduction to Digital Communication'. 2nd edition. 2000. Prentice Hall.